Downloaded from https://www.lyellcollection.org by UK Research and Innovation (UKRI/BGS/BAS) on Aug 13, 2025

Research article

Geoenergy

https://doi.org/10.1144/geoenergy2024-027 | Vol. 3 | 2025 | geoenergy2024-027

Structural controls on pressure communication across the Bunter Sandstone Formation, UK Southern North Sea

L. E. Abel[1]*, J. D. O. Williams[1], K. A. Wright[2], T. A. Randles[2], P. Bridger[1], H. A. Morris[1], T. J. H. Dodd[2], G. E. Plenderleith[2] and J. C. White[1]

[1] British Geological Survey, Nicker Hill, Keyworth, Nottingham NG12 5GG, UK
[2] British Geological Survey, The Lyell Centre, Research Avenue South, Edinburgh EH14 4AP, UK
LEA, 0009-0006-4109-0163; JDOW, 0000-0003-0177-9848; KAW, 0000-0002-5906-6368; TAR, 0000-0001-6428-5138; PB, 0000-0002-1513-0559; HAM, 0009-0003-3912-8423; TJHD, 0000-0003-2257-6740; GEP, 0000-0002-2311-3863; JCW, 0000-0001-8227-0677
* Correspondence: luab@bgs.ac.uk

Abstract: The utilization of extensive saline aquifers for CO_2 storage will require careful consideration of the potential pressure responses. The displacement of formation waters results in far-reaching pressure footprints that extend beyond the storage sites. Where multiple storage projects share a connected saline aquifer, the available pressure budgets for neighbouring projects may be negatively impacted. Structures such as faults and salt walls can potentially divide an aquifer into smaller hydraulic units.

The extent of hydraulic units in the Bunter Sandstone Formation (BSF) within the UK Southern North Sea (UKSNS) was investigated by structural interpretation of seismic data. A new classification scheme was developed to characterize the major structural features affecting the BSF and their likely impact on boundary conditions. The resultant boundary condition map indicates where structures are expected to inhibit pressure communication through displacement/dislocation of the BSF aquifer. The results were validated by pressure data, which confirmed the existence of variable pressure regimes across the BSF.

Understanding these boundary conditions is essential to support the strategic deployment of CO_2 storage in the UKSNS and to maximize storage capacity. The methodology can also be applied to other regions where extensive saline aquifers are considered for CO_2 storage.

Received 28 August 2024; **revised** 17 January 2025; **accepted** 24 February 2025

Carbon Capture and Storage (CCS) will be an important technology to enable the reduction of greenhouse gas emissions from power generation and industrial processes where emissions are otherwise hard to abate (CCC 2020). To meet its obligations in the Sixth Carbon Budget, the UK government's Department for Energy Security and Net Zero (DESNZ) estimates that CO_2 injection rates of at least 50 Mt of CO_2 per year will be needed in 2035 (DESNZ 2023). The estimated required injection rates increase during the Seventh Carbon Budget (2038–42), and 90–170 Mt CO_2 storage per year will be required by 2050 (DESNZ 2023).

Depleted gas fields and saline aquifer formations in the UK Southern North Sea (UKSNS) provide storage opportunities for CO_2 captured from industrial clusters in eastern England. The Lower Triassic Bunter Sandstone Formation (BSF), the youngest formation of the Bacton Group, contains several large anticlinal and periclinal structures that form attractive prospects for CO_2 storage, with the potential to provide gigatonne-scale storage capacity (Holloway *et al.* 2006; Bentham *et al.* 2014). To date, carbon storage licences have been awarded over large parts of the UKSNS (Fig. 1), with the BSF saline aquifer forming the principal target for CO_2 storage at several sites (Furnival *et al.* 2014; Hollinsworth *et al.* 2022).

Numerical simulation studies have sought to evaluate the dynamic behaviour of industrial-scale CO_2 injection in the BSF (Smith *et al.* 2011; Heinemann *et al.* 2012; Noy *et al.* 2012; Williams *et al.* 2013; Agada *et al.* 2017; Kolster *et al.* 2018). While CO_2 is expected to remain trapped locally within the targeted structural closures, these studies have highlighted that regional pressurization of the formation may occur due to injection. Displacement of brine results in an extensive pressure footprint that can impact areas of the aquifer many tens of kilometres beyond the storage sites themselves. To avoid unanticipated pressure increases, the risk of pressure perturbations should be considered carefully, especially where multiple CO_2 injection projects share connected saline aquifers (Shoulders and Hodgkinson 2024).

The risk of pressure communication between separate storage projects will require proactive risk management and collaboration between different storage operators and regulatory agencies. Assessing the controlling factors at the earliest opportunity will help to facilitate the strategic development of the BSF as a nationally important subsurface resource.

Across the UKSNS, large-scale structural lineaments, such as the Dowsing Graben System and the salt walls bounding the Sole Pit High (Fig. 1), have previously been inferred to divide the Lower to Middle Triassic strata into large structural compartments that are likely to control the extent of pressurization across the basin (Smith *et al.* 2011; Noy *et al.* 2012). However, there have been few detailed studies that document and explore how these structures might affect hydraulic connectivity within the BSF. Consequently, there is inadequate information to aid in defining boundary conditions for geocellular modelling and numerical simulation studies for CO_2 injection. An improved understanding of the structural boundaries across the UKSNS is essential to support successful and efficient deployment of geological CO_2 storage in the region.

This study aims to address this issue by using a regional 2D and 3D seismic reflection database to evaluate the role of the large-scale structural lineaments in controlling regional aquifer connectivity within the BSF. A classification scheme is devised to characterize the structural features that are likely to control pressure communication between adjacent hydraulic units. The scheme is then applied to the major structural boundaries identified in the UKSNS to develop a boundary condition map that summarizes the degree of connection, or disconnection, of the Bacton Group across the

© 2025 British Geological Survey. This is an Open Access article distributed under the terms of the Creative Commons Attribution License (http://creativecommons.org/licenses/by/4.0/). Published by The Geological Society of London for GSL and EAGE. Publishing disclaimer: https://www.lyellcollection.org/publishing-hub/publishing-ethics

Downloaded from https://www.lyellcollection.org by UK Research and Innovation (UKRI/BGS/BAS) on Aug 13, 2025

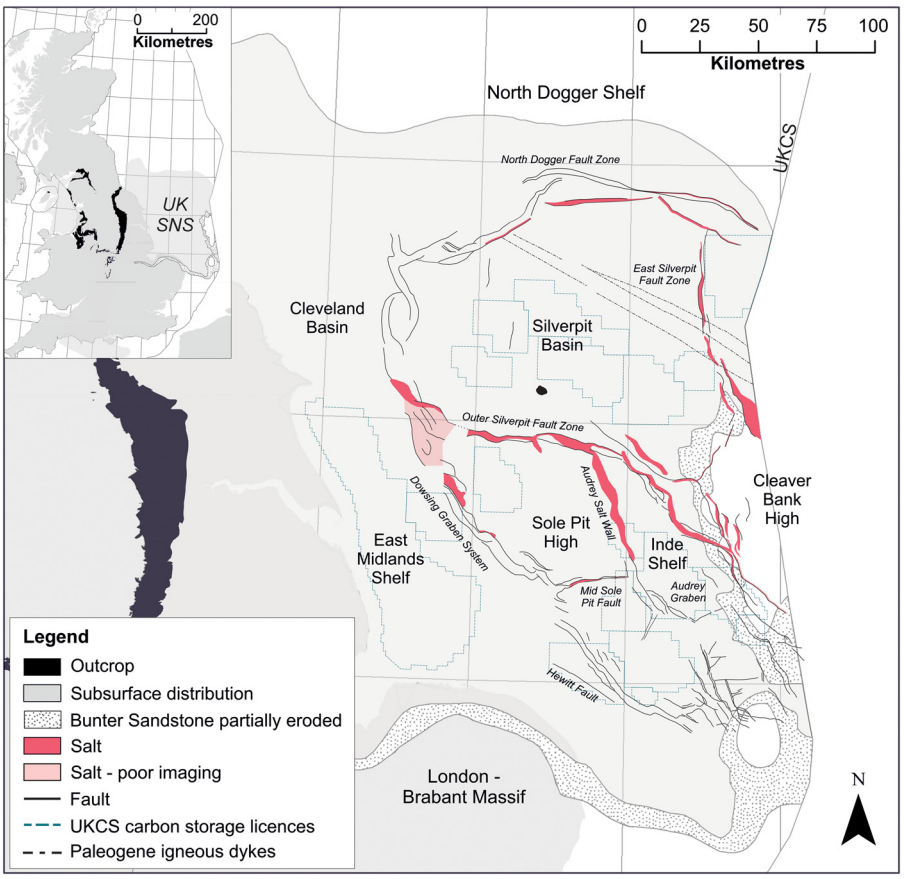

Fig. 1. Location of study region and structural map showing major fault and salt wall features at top Bunter Sandstone Formation (BSF) level, as derived from this study. The BSF extent, erosional margins and onshore outcrop are taken from Cameron *et al.* (1992). Offshore quadrant, carbon storage licence and coastline linework contain information provided by the North Sea Transition Authority and/or other third parties. UKCS, UK Continental Shelf.

structural features of interest. While the utility of the approach is demonstrated through its application to the BSF of the UKSNS, the methodology can equally be applied to other regions where extensive saline aquifer formations are considered for CO_2 storage.

Geological setting

The UKSNS is situated at the western extent of the E–W-orientated Southern Permian Basin that once extended across Europe to Poland (Doornenbal and Stevenson 2010). It comprises a series of basins and structural highs that have been investigated extensively, primarily through oil and gas exploration, and are now of interest to a range of energy transition technologies including CCS (Doornenbal and Stevenson 2010; Heinemann *et al.* 2012; Doornenbal *et al.* 2022; Underhill *et al.* 2023). The generalized stratigraphy is summarized in Figure 2.

Basin fill was initiated when thermal subsidence provided accommodation for deposition of the Leman Sandstone Formation, which forms part of the Lower Permian Rotliegend Group (Glennie and Boegner 1981; Glennie 1990; Doornenbal and Stevenson 2010). Aeolian and fluvial sands were deposited in a desert environment over a partially eroded substrate of Carboniferous and older rocks. This gave way to lacustrine conditions in the northern UKSNS, where the Leman Sandstone Formation interdigitates with the Silverpit Formation (Cameron *et al.* 1992). Higher rates of subsidence occurred in the Sole Pit Basin (subsequently inverted in the Late Cretaceous to form the Sole Pit High) (Figs 1, 2), with the axis of the main depocentre rotated *c.* 30° clockwise to the trend of the earlier NW–SE inversion structures of the Variscan Orogeny (Glennie and Boegner 1981; Cameron *et al.* 1992).

Continued thermal subsidence throughout the Permian resulted in the UKSNS lying *c.* 250 m below global sea-level (Smith 1979; Cameron *et al.* 1992). A rise in eustatic sea-level and subsidence of the Norwegian–Greenland Sea rift (Proto-Atlantic fracture zone) enabled the southward transgression of the Arctic Seas (Ziegler 1988; Cameron *et al.* 1992; Pharoah *et al.* 2010). This resulted in flooding of both the Northern and Southern Permian basins and deposition of the Zechstein Group (Ziegler 1988; Glennie 1990; Stewart and Coward 1995). The Zechstein Group comprises a cyclical carbonate–evaporite sequence deposited in a partially restricted marine environment. Within the UKSNS, the Zechstein Group has been subdivided into five cycles, Z1 to Z5, controlled by fluctuations in sea-level (Smith 1979; Grant *et al.* 2019*b*; Fyfe and Underhill 2023*a*, *b*). The deposition of thick evaporite deposits affected subsequent deformation mechanisms within the UKSNS by decoupling deformation of the pre- and post-salt strata (Van Hoorn 1987; Allen *et al.* 1994; Coward and Stewart 1995; Brennan and Adam 2023; Brennan *et al.* 2023) and therefore exerted an important control on the present structural configuration of the UKSNS (Cameron *et al.* 1992).

A return to terrestrial conditions marked the start of Triassic sedimentation. Arid to semi-arid conditions prevailed across the basin during the Early Triassic. Deposition of the Bacton Group commenced with distal floodplain and lacustrine mudstones of the Bunter Shale Formation, which attains thicknesses of up to *c.* 400 m in the central part of the UKSNS (Cameron *et al.* 1992). Fluvial sandstone facies are increasingly interdigitated with lacustrine facies in the upper part of the Bunter Shale Formation towards the present-day coastline (Fig. 1). Sandstones of the overlying BSF were mainly deposited by fluvial processes, with sediments sourced primarily from the south and SW via the Triassic river drainage system (McKie and Williams 2009; Newell 2018). The thickest accumulations of sandstone occurred in the Sole Pit Basin (up to *c.* 350 m), indicating continued generation of accommodation space during deposition of the BSF (Cameron *et al.* 1992). The BSF is overlain by the Haisborough Group, which predominantly comprises red mudstones, with thin dolomite and anhydrite beds, and widespread halite members. The earliest marine incursion resulted in deposition of the

Downloaded from https://www.lyellcollection.org by UK Research and Innovation (UKRI/BGS/BAS) on Aug 13, 2025

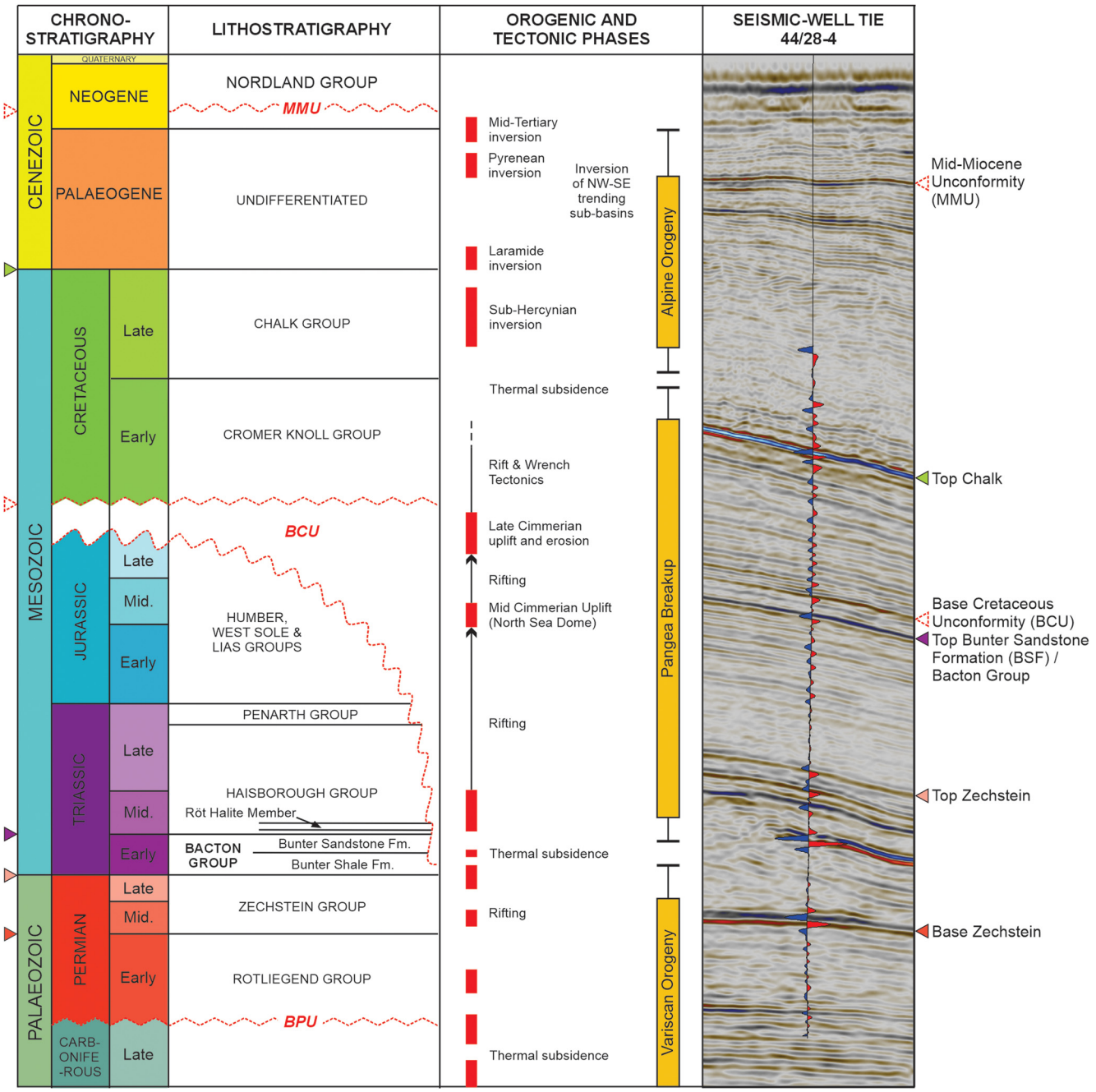

Fig. 2. Tectonostratigraphic chart with seismic-well tie for Well 44/28-4. The seismic picks are shown for each of the main seismic horizons interpreted: Base Zechstein, Top Zechstein, Top Bacton Group, Base Cretaceous Unconformity (BCU), Top Chalk and Mid-Miocene Unconformity (MMU), on both the seismogram and the chronostratigraphic column. The colour scheme used throughout follows that defined by the International Commission on Stratigraphy (Cohen *et al.* 2013). Contains information provided by the North Sea Transition Authority and/or third parties. Source: the tectonic history was compiled from Glennie (1990), Pharoah *et al.* (2010) and Grant *et al.* (2019*a*, 2020).

Röt Halite Member (Fig. 2), a predominantly halite-bearing unit up to *c.* 100 m thick, which forms a top seal for several prospective BSF storage sites (Heinemann *et al.* 2012; Williams *et al.* 2014).

The Viking and Central Graben to the north/NE (Patruno *et al.* 2022) developed owing to extensional faulting initiated during the Mid Triassic (Pharoah *et al.* 2010). Reactivation of the Variscan basement during the Early–Mid Triassic also contributed to thickness variations within Triassic strata, with the Sole Pit Basin remaining the main depocentre in the UKSNS (Stewart and Coward 1995). Salt mobilization was controlled largely by the pre-salt structural configuration and the increased thickness of salt into the UKSNS across the Dowsing Fault Zone (Underhill 2009). Gravitational sliding towards the basin centre initiated halokinesis (Stewart and Coward 1995). Both the Dowsing Graben System and the North Dogger Fault Zone are understood to have resulted from the mobilization of the Zechstein salt within the UKSNS (Allen *et al.* 1994; Griffiths *et al.* 1995; Grant *et al.* 2019*a*, 2020). As salt-cored anticlines, periclines and diapirs started to form, the overlying Triassic units were folded, localizing subsequent deposition, which in turn encouraged further diapirism in response to sediment loading. This folding in the centre of the UKSNS resulted in overall shortening of the post-salt cover rocks (Griffiths *et al.* 1995). To accommodate this shortening, extension along both the Dowsing Graben System and the North Dogger Fault Zone continued, resulting in the formation of large graben systems and zones of separation within the BSF along these margins (Grant *et al.* 2019*a*, 2020). The Dowsing Graben System developed over the pre-existing basement fault system known as the Dowsing Fault Zone.

Downloaded from https://www.lyellcollection.org by UK Research and Innovation (UKRI/BGS/BAS) on Aug 13, 2025

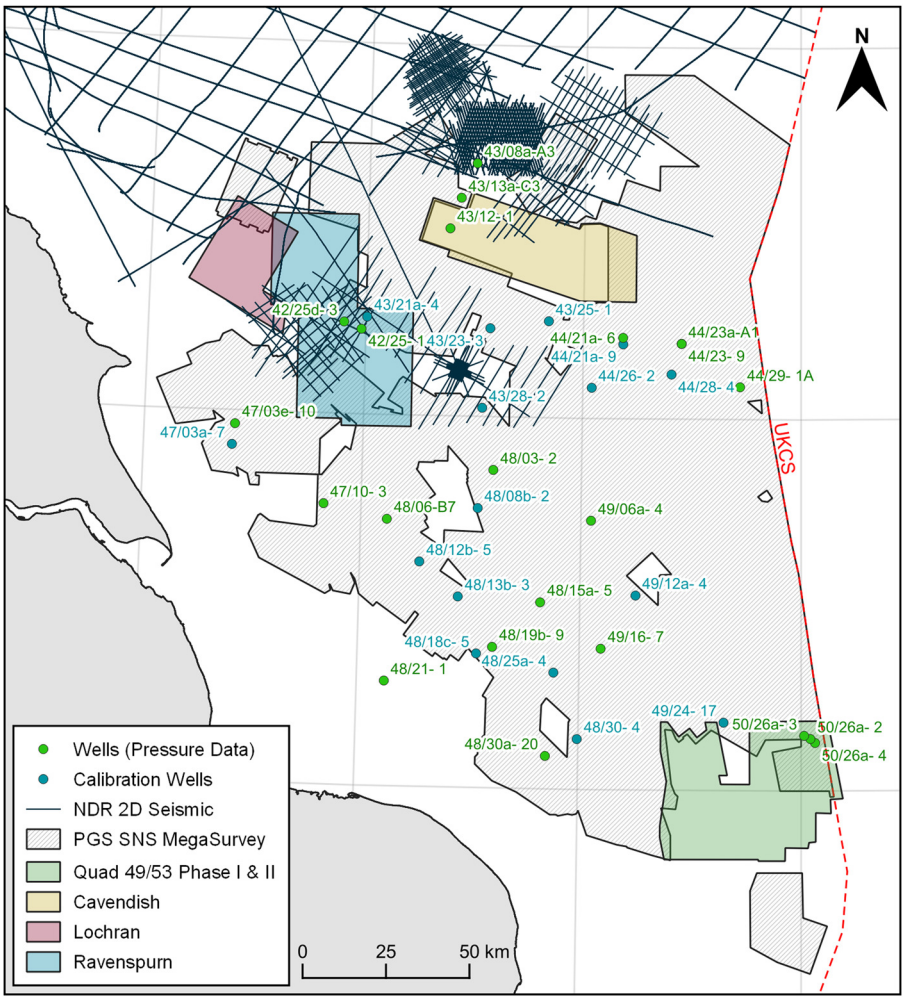

Fig. 3. Overview of the subsurface dataset used in this study. UKCS, UK Continental Shelf: this defines the extent of UK waters. With the exception of the Cavendish, Ravenspurn and Quad49/53 Phase I & II 3D seismic datasets, all data are publicly available through the National Data Repository (NDR). Offshore quadrant, coastline and seismic data outline linework contains information provided by the North Sea Transition Authority and/or other third parties.

Continued rifting of the Central Graben in the Early Jurassic, combined with both regional thermal subsidence and a rise in eustatic sea-level, led to the development of a shallow-marine environment in the UKSNS (Pharoah *et al.* 2010). The topography generated by salt mobilization resulted in variable thicknesses and lithologies of Jurassic-aged sediments (Cameron *et al.* 1992). Regionally, the Jurassic-aged units comprise mainly mudstones and argillaceous limestones of the Lias Group, fluviodeltaic mudstones and sandstones of the West Sole Group, and a mud-dominated succession of the Humber Group (Cameron *et al.* 1992; Lott and Knox 1994). The Jurassic succession is observed to thicken into the hanging walls of faults, adjacent to salt withdrawal features and diapirs, and into the Dowsing Graben System (Van Hoorn 1987; Cameron *et al.* 1992; Stewart and Coward 1995; Pharoah *et al.* 2010). Preservation of Jurassic strata is variable across the UKSNS, which is interpreted to be due largely to subsequent erosion beneath the Base Cretaceous Unconformity (BCU). Late Cimmerian tectonic activity, which initiated in the Late Jurassic, resulted in significant uplift and erosion in the UKSNS, removing much of the Jurassic interval across the basin. In the Silverpit Basin, Jurassic sediments have mostly been removed beneath the BCU (Coward and Stewart 1995). The BCU cuts down through Jurassic and Triassic strata into the BSF over the Cleaver Bank High (Fig. 1) in the eastern part of the UKSNS.

Rifting and salt migration continued during the Early Cretaceous resulting in syndeposition of Cretaceous strata. The UKSNS was situated in a marine environment that extended across the Southern Permian Basin and was connected to the Atlantic via the Viking Graben (Cameron *et al.* 1992). Eustatic sea-level rise led to a decrease in terrestrial material in the UKSNS and allowed for chalk deposition in areas of earlier uplift and erosion.

During the Early Cretaceous and into the Early Cenozoic, north–south compression affected the UKSNS during the Sub-Hercynian and Alpine orogenic phase, leading to reactivation, inversion and dextral movement along existing NW–SE-trending structures. This resulted in inversion of the Sole Pit Trough, which was uplifted to create the Sole Pit High. It is estimated that up to 2 km of erosion occurred by the Late Cretaceous, with no preservation of strata younger than the Jurassic over the High (Bulat and Stoker 1987; Van Hoorn 1987; Cameron *et al.* 1992; Japsen 2000; Pharoah *et al.* 2010). Inversion continued throughout the Cenozoic during three distinct phases (Fig. 2); each phase has a variable impact on the UKSNS sub-basins. Halokinesis continued into the Cenozoic, with migration of Zechstein evaporites influencing deposition of Cenozoic strata (Cameron *et al.* 1992). Cenozoic syndepositional packages are observed around faults and salt structures in the NE of the UKSNS (Underhill *et al.* 2009). Thermal subsidence occurred throughout the UKSNS along the axis of the North Sea Rift System. This resulted in tilting of the UKSNS eastwards and greater deposition of the Cenozoic units towards the median line (Pharoah *et al.* 2010).

Data and methods

Seismic database

This study utilizes a regional 2D and 3D seismic and well database to map, characterize and classify the major regional structural boundaries in the UKSNS. The PGS 2015 SNS MegaSurvey post-stack 3D dataset extends across much of the area (Fig. 3). Additional 2D and 3D data were sourced from Schlumberger (SLB) and the

Downloaded from https://www.lyellcollection.org by UK Research and Innovation (UKRI/BGS/BAS) on Aug 13, 2025

National Data Repository (NDR) to provide further coverage. A full listing of the seismic data used in this study is provided in Table 1.

Mis-ties between the 2D and 3D surveys were corrected where possible, with the SNS MegaSurvey used as the reference dataset. However, it was not possible to correct residual mis-ties within the SNS MegaSurvey volume where different surveys have been merged. Varying processing and acquisition parameters used across the different vintages of data, both within the SNS MegaSurvey and the additional 2D and 3D datasets, resulted in difficulty in attaining precise alignment across the full data catalogue. These artefacts do not negatively impact the characterization of regional structural boundaries and as such do not affect the outcomes of the study.

The study leveraged existing British Geological Survey seismic interpretations from the UKSNS. These interpretations were collated from a number of historical project archives, including interpretations developed for different purposes by various practitioners over many years. A mixture of 2D and 3D interpreted horizons were available for the Base Zechstein, Top Zechstein, Top BSF/Top Bacton Group, BCU, Top Chalk and Mid-Miocene Unconformity (MMU). For purposes of quality control, seismic-well ties were generated for 16 calibration wells (Fig. 3). The following selection criteria were used to select wells for the analysis: the wells have relatively vertical trajectories; checkshot data are available from near-seabed to total depth; the wells are located within the MegaSurvey seismic data extent; and they are in areas with relatively simple structural configurations. The seismic-well tie workflow comprised sonic calibration and synthetic seismogram generation, using a standard Ricker wavelet with a frequency of 25 Hz, sample rate of 4 ms and length of 128 ms. An example of a typical synthetic seismogram is shown alongside the generalized stratigraphic column in Figure 2. Where required, the horizons were reinterpreted following well correlation. Revisions were focused on the areas adjacent to the principal structural features affecting the BSF shown in Figure 1, which are referred to here as structural boundaries. This structural linework was derived from the interpreted Top BSF horizon and provides the basis for application of the classification scheme presented in this study.

Classification scheme

A classification scheme was developed to allow the attribution of appropriate boundary conditions in dynamic models of CO_2 storage. In this scheme, each structural boundary within the study area was categorized according to the geometric relationship and style of separation of the Bacton Group across the structure. The Bacton Group is interpreted as a single unit in the dataset because the base of the BSF could not be mapped with confidence across the region. Two key factors influence this lack of imaging. First, a clear acoustic impedance contrast between sandstone of the BSF and mudstones of the underlying Bunter Shale Formation is hindered by the presence of transitional depositional facies at the boundary. Second, the seismic imaging of the base BSF is hampered by the low signal to noise ratio, migration artefacts associated with the flanks of the anticlines and lack of a clear amplitude response. A benefit of this approach is that the juxtaposition mapping accounts for any uncertainty related to BSF thickness variations and uncertain petrophysical properties of the underlying Bunter Shale.

The classification scheme comprises three end members and four intermediary categories (Fig. 4), with end members describing: (1) a connected reservoir with no lateral or vertical separation of the Bacton Group; (5) faulted boundaries with complete disconnection and no self-juxtaposition; and (7) complete disconnection of the Bacton Group by salt structures. Intermediary categories (2) to (4) represent conditions where the Bacton Group is self-juxtaposed across significant fault structures or zones of salt-induced deformation. Categories (3) and (6) comprise combinations of faulting and salt-induced deformation such as reactive salt structures associated with faulting.

Interpretation method

The major structures were first identified from published structural maps of the UKSNS (Glennie and Boegner 1981; Van Hoorn 1987; Cameron *et al.* 1992; Allen *et al.* 1994; Stewart and Coward 1995; Doornenbal and Stevenson 2010; Grant *et al.* 2019*a*, 2020; Brennan and Adam 2023). A variance map was then created for the Top BNS (Top Bacton Group) to validate which structures intersect the Bacton Group and to map their locations (Fig. 1). A detailed evaluation was undertaken along each of the structural boundaries to enable classification. This was achieved through visual inspection of a seismic cross-section generated perpendicular to the boundary where data would allow. Each structure was systematically assessed at regular intervals, by moving the section along-strike at an approximate spacing of 2000 m. Shorter intervals were used where appropriate based on the complexity of the structure, data presence and quality. Where 3D data were not present, the orientation of the section was contingent on availability of 2D seismic lines.

Table 1. Seismic data interpreted during this study

CS9 name	Survey description	Data owner	Type
TT922D0004	0043/28 1992	Total	2D
AT872D1005	A48/18C-87-1-26	BP	2D
AT912D0005	AR43/10-91-01-19	BP	2D
AM852D1010	AUK85T-771-819 43/2	BP	2D
AM912D0003	AUK91AF 071-079 43/7	BP	2D
BB922D1001	B92-43	NHDA	2D
BP832D1002	BP83-1001-1025 42/24,25	BP	2D
GE943F0001	Cavendish 3D	SLB	3D
ET852D1004	E85D	Shell	2D
RD123D4218	Lochran 3D	INEOS	3D
WG842D1004	Mid North Sea Survey	SLB	2D
WG152D0002	Mid-North Sea High OGA	NSTA	2D
GE933F0001	Quad 49/53 Phase I & II	SLB	3D
WG973F0004	Ravenspurn OBC 1998 3D	SLB	3D
	SNS MegaSurvey	PGS	3D
CN892D1016	UK_CON89_C4389_00	ConocoPhillips	2D

NHDA, National Hydrocarbons Data Archive; SLB, Schlumberger; NSTA, North Sea Transition Authority.

Downloaded from https://www.lyellcollection.org by UK Research and Innovation (UKRI/BGS/BAS) on Aug 13, 2025

The overall character of each boundary was considered, and any marked changes in structural style along the boundary were noted as per the classification scheme (Fig. 4). Each boundary was classified according to the predominant structural style observed at Bacton Group level. Salt deformation is typically accompanied by faulting, and so, for characterization purposes, the most dominant structures that are likely to affect connectivity across the Bacton Group were used. For example, where a salt wall is developed along a fault, resulting in complete lateral separation of the Bacton Group, the boundary segment was classified as Class 7. In areas of uncertainty or poor data quality, classification was based on the best judgement of the interpreter. A conservative approach was taken by applying Classes 2, 3 or 4 to represent potential connectivity in areas of uncertainty. An example of a typical structure for each of the classification scheme categories is shown in Figure 5.

The classification is based on geometric relationships across the major structural lineaments and can therefore be used to infer the degree of connectivity (or otherwise) across the structures of interest. Based on an empirical assessment of the estimated flow properties of the bounding structures, this scheme was simplified into three categories, as shown in Figure 4. This simplification defines the reservoir boundary connectivity as connected, possibly connected or disconnected, irrespective of structural style. This simplified scheme provides boundary condition information for numerical flow modelling while the detailed scheme informs characterization requirements for project developers, for example, fault seal analysis. The resulting classification scheme has been applied to the SNS structures shown in Figure 1 that intersect the BSF.

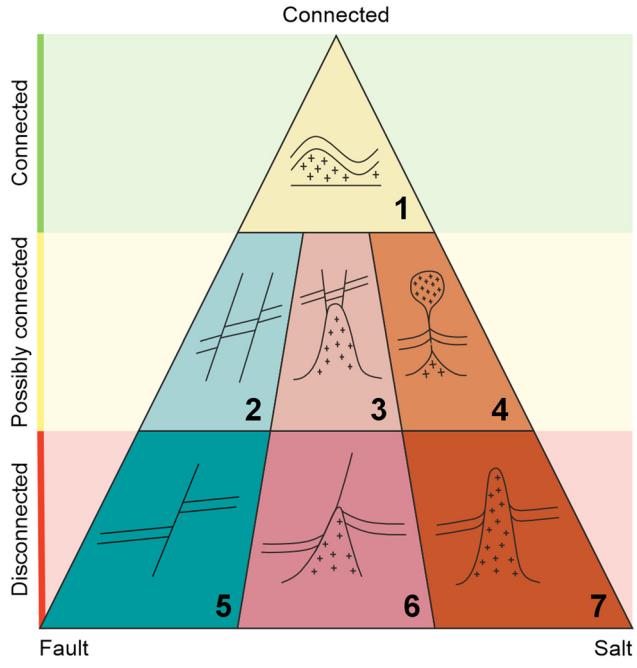

Fig. 4. Boundary classification scheme. The geometric relationships of the Bacton Group across the structures are categorized by structural style within the tertiary diagram: 1, connected – no vertical or lateral separation; 2, faulted with self-juxtaposition; 3, juxtaposition due to faulting and salt deformation; 4, salt deformation with juxtaposition; faulting also occurs where there is salt deformation with a degree of juxtaposition; 5, faulted – complete separation with no juxtaposition; 6, complete separation by combination of salt and faulting; 7, salt – complete lateral separation by salt. A simplified scheme that classifies the boundaries according to the degree of connectivity irrespective of structural style is shown on the left-hand side: green, connected; yellow, possibly connected; red, disconnected.

Pressure data

To determine the pore pressure gradients across the UKSNS, wells where pressure measurements had been taken within the BSF were identified from well records obtained from the NDR (Fig. 3). As the objective was to identify any variations in the pressure regime in different parts of the basin, it was necessary to remove the effects of local hydrocarbon accumulations and any gas production artefacts, such as pressure depletion effects. This was achieved by first plotting the pressure measurements against true vertical depth to differentiate between water and gas column measurements and to identify anomalous values. In some cases, gas water contact depths were identified on company logs/reports available from the NDR, readily enabling validation. Following removal of gas column measurements, remaining measurements from wells exhibiting erratic or anomalously low values were reviewed to evaluate if pressures might have been impacted by gas production activities. This included a review of the proximity and timing of the measurements in relation to gas production activities in the BSF. This ensured that only unperturbed measurements within the saline aquifer were used for further analysis of regional pressure gradients. The final pressure database comprised 142 measurements from a total of 22 wells. The data comprise pressure measurements from wireline tester, drill stem tests and a single driller's estimate. The driller's estimate, from well 49/06a-4 in the northern part of the Inde Shelf, is the estimated pressure made by the driller based on assessment of the drilling exponent (Dxc), flowline temperature and shale density, which were used to detect any changes from the established normal pore pressure trend (as reported in the well completion report). Despite not representing a true pressure measurement and noting the associated uncertainty, the reported estimate was included in the dataset because no BSF pressure measurements were found from other wells in this part of the basin.

Evaluation of the structural boundaries in the UKSNS

Each of the key structural boundaries identified within the Bacton Group is described and discussed in this section. The boundaries have been assessed according to the classification scheme shown in Figure 4, by visually evaluating the geometric relationship between the Bacton Group strata on each side of the structural features. Figure 6 shows the location of all cross-sections.

Dowsing Graben System

The NW–SE-orientated Dowsing Graben System defines the boundary between the Cleveland Basin (Fig. 1), East Midlands Shelf and South Hewett Shelf to the west, and the Silverpit Basin and Sole Pit High to the east (Fig. 6). Figure 5e shows an example of the typical structural geometries observed along the boundary. Although the orientation of the Dowsing Graben System is inherited from the underlying Dowsing Fault Zone, the deformation affecting the BSF is decoupled from the basement structure by the presence of thick Zechstein evaporite sequences. The boundary comprises a series of graben and half graben bound by listric growth faults that detach into the Zechstein salt, as illustrated in Figure 5e. These are regionally extensive and are mainly hard linked in the transfer zones between graben. The evolution of the Dowsing Graben System is detailed in Kyari (2018) and Grant *et al.* (2019*a*). Within the graben themselves, the Bacton Group strata are predominantly absent; however, in the transfer zones between the graben in the north of the Dowsing Graben System, it is less clear if some isolated Bacton Group strata remain. Accurate interpretation along some sections of the boundary is hampered by variable data availability and resolution within these structurally complex zones. This is also

Downloaded from https://www.lyellcollection.org by UK Research and Innovation (UKRI/BGS/BAS) on Aug 13, 2025

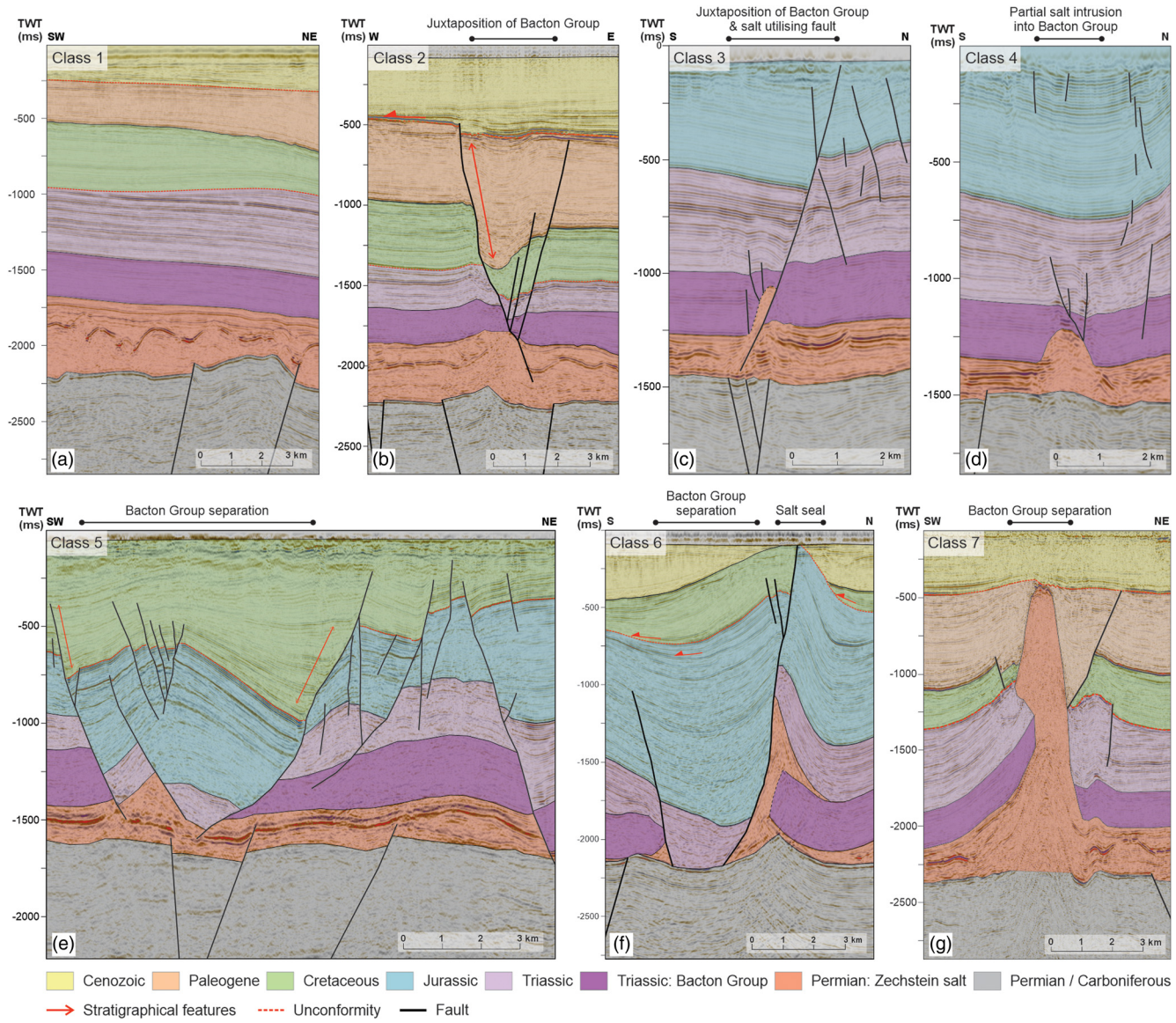

Fig. 5. Example sections for each class of the classification scheme. These sections show the classification based on the geometric relationship of the Bacton Group strata across the boundary. The location of each section is shown in Figure 6. (**a**) Connected – no vertical or lateral separation of the Bacton Group. (**b**) Faulted with self-juxtaposition. (**c**) Juxtaposition due to faulting and salt deformation. (**d**) Salt deformation with juxtaposition; faulting also occurs where there is salt deformation with a degree of juxtaposition. (**e**) Faulted – complete separation with no juxtaposition. (**f**) Complete separation by combination of salt and faulting. (**g**) Salt – complete lateral separation by salt. Contains information provided by the North Sea Transition Authority and/or third parties.

the case where major E–W-striking fault systems such as the Flamborough Head Fault Zone terminate at the Dowsing Graben System. Isolated sections of the Bacton Group can be identified in the seismic data within these junctions, although they are not laterally persistent. It is expected that they are confined to isolated horst structures that are surrounded by zones of separation, and so it is inferred that the Bacton Group is disconnected across the Dowsing Graben System.

The zones of separation of the Bacton Group strata can be up to 5 km wide. Consequently, pressure communication across the Dowsing Graben System is deemed unlikely on typical operating timeframes (decadal) for CO_2 storage projects. Most of the boundary is defined as Class 5. Some variation is observed along the length of the Dowsing Graben System, with salt intrusion present within some sections changing the categorization to Class 6 or 7 dependent on the dominant local style of disconnection. This is particularly evident where the Outer Silverpit Fault Zone intersects the Dowsing Graben System, where there is an increased presence of salt within the bounding faults.

North Dogger Fault Zone

The North Dogger Fault Zone defines the northern margin of the Silverpit Basin. This fault zone can be separated into two sections: (1) a WNW–ESE-orientated listric fault and (2) a SW–NE-transtensional graben system. These faults, along with the Dowsing Graben System, balance the halokinetic shortening (folding) observed in the post-Zechstein cover in the central UKSNS. Seismic data coverage is less extensive along this part of the boundary, with a 3D seismic dataset available for the eastern and western margins of the fault system, and 2D datasets providing additional infilling coverage (see Fig. 3).

The WNW–ESE-orientated bounding fault (Fig. 7) forms a southward-dipping listric fault that soles-out in the Zechstein Group. Antithetic faults and splays are present along some sections of the main listric fault. Parallel to this, a salt-cored rollover anticline is present adjacent to the fault. Two salt walls, orientated oblique to the main fault, converge towards the centre of the structure (Fig. 1). These structures vary in size and geometry along their respective

Downloaded from https://www.lyellcollection.org by UK Research and Innovation (UKRI/BGS/BAS) on Aug 13, 2025

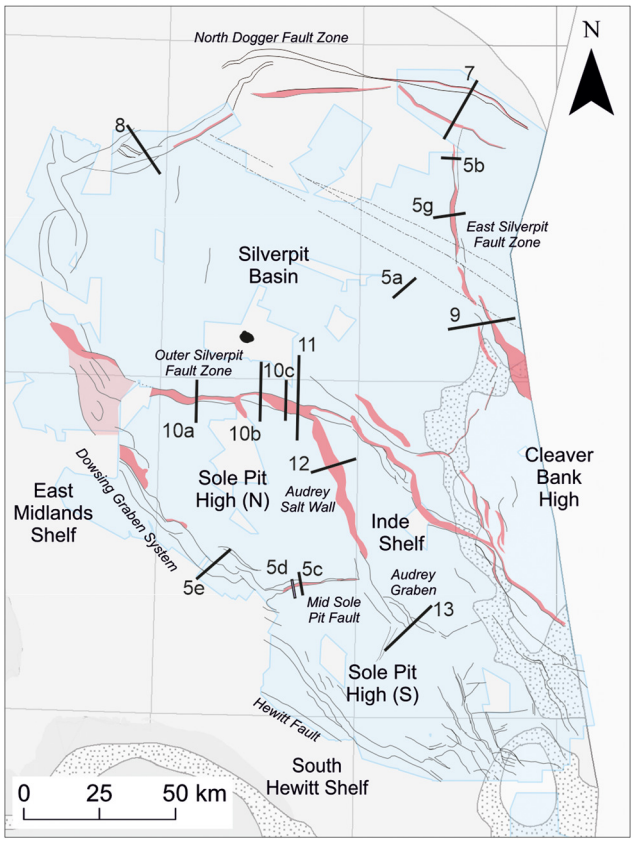

Fig. 6. Cross-section locations. The bold lines indicate the location of all cross-sections presented, with the corresponding figure number identified. The blue polygon outlines the extent of the 3D seismic datasets. For legend, see Figure 1. Source: the extent of the Bunter Sandstone Formation and the erosional margins are taken from Cameron *et al.* (1992), and the offshore quadrant, coastline and seismic data outline linework contains information provided by the North Sea Transition Authority and/or other third parties.

lengths. Middle to Upper Triassic strata are only present in the hanging wall directly adjacent to the North Dogger Fault Zone (Fig. 7). A significant thickness of the Triassic succession is removed beneath the BCU. The consistency in thickness of the Bacton Group indicates that the major period of faulting occurred post-Early Triassic. Displacement of Lower Cretaceous strata occurs only along short sections of the fault. It is interpreted that this only occurs in the main depocentres where larger displacements are present. The North Dogger Fault Zone becomes less listric towards the WNW and is soft linked with faults at the level of the Rotliegend Formation (Lower Permian). The variation in throw and the dip angle of the faults (Fig. 1) suggests that two faults may have linked to form the single throughgoing fault; Griffiths *et al.* (1995) also noted the change in the geometry of this fault zone.

Faulting associated with the salt walls extends upwards into the Cenozoic-aged strata above, implying that halokinesis continued into the Neogene (Fig. 7). This is evident from the displacement seen at the unconformity separating the Paleogene and Neogene strata; this is here (and indeed previously) assumed to be the MMU (*sensu* Patruno *et al.* 2022).

Compression is observed in the hanging walls of faults associated with the salt walls adjacent to the North Dogger Fault (Fig. 7). Onlapping geometries are observed within Paleogene strata over the anticline above the North Dogger Fault, suggesting that compression (possibly related to inversion) occurred during the Mid to Late Paleogene. There is a slight anticlinal trend observed within the Lower Neogene strata, suggesting folding continued beyond the Paleogene. In contrast, extensional faulting remains within the Neogene-aged strata, particularly within areas that directly overlie salt walls. This is indicated by the offset of reflectors and an increase in sediment thickness in the hanging wall. Remobilization of the salt may account for the extensional movement.

Faulting along the WNW–ESE section of the North Dogger Fault Zone has resulted in *c.* 2.5 km of lateral separation of Bacton Group strata. The deformation resulting from salt intrusion at the obliquely orientated salt wall separates the Bacton Group strata by *c.* 1 km. This lateral displacement and lack of cross-fault self-juxtaposition suggests that hydraulic communication across the structures is unlikely. The structural variability along the North Dogger Fault Zone means that there is variability in terms of the classification assigned. Different sections of the structure were categorized as Class 5, 6 or 7 depending on the influence of mobile salt within the structure and mapped on to the regional structure map.

In contrast, the SW–NE-transtensional graben system resembles the structural geometry of the Dowsing Graben System (Fig. 8). Faulting initiated following deposition of the Bacton Group strata, and the faults detach into the Zechstein salt. Zones of separation at Bacton Group level are observed within the graben. Although the fault geometries are variable along the boundary, the zone of separation remains present. Erosion has removed much of the Cenozoic-aged strata in the western extent of the structure; however, moving northeastwards, the MMU is observed, and Neogene strata are present. Faults on the southern boundary of the graben remained active into at least the Neogene, potentially extending up to the present-day seabed. The northern boundary fault shows decreasing displacement towards the NE where it terminates at subcrop to the BCU. In places along the boundary fault, salt intrusion adjacent to the fault planes is observed and interpreted in the 3D seismic data; in these locations the structural boundary is categorized as Class 6.

East Silverpit Fault Zone

The N–S-orientated feature that divides the eastern extent of the Silverpit Basin is termed the East Silverpit Fault Zone (Fig. 5b, g). The structure is referred to as the Dogger Fault Zone by Cameron *et al.* (1992) but is termed the East Silverpit Fault Zone here to provide clear differentiation from the North Dogger Fault Zone.

The geometries observed along the East Silverpit Fault Zone are highly variable along-strike. The deformation style changes rapidly, alternating between salt intrusion (salt walls, diapirs and rollers) and faulting, with complex intersections. The northern extent of the boundary is characterized by an eastward-dipping normal fault that offsets the Bacton Group to form a half graben, with little salt present within the structural boundary (Fig. 5b). The degree of displacement varies along-strike, with the Bacton Group self-juxtaposed in places. A reactive salt roller is present in the footwall along some sections of the fault. The influence of salt increases towards the south, and the roller increases in size, eventually forming a series of narrow salt walls (Fig. 5g). This results in uplift of the overburden and complete disconnection of the Bacton Group. The salt walls are divided by zones of reduced salt intrusion and increased faulting.

As the salt walls begin to deplete to the south, faulting becomes the dominant structural boundary style, and the Bacton Group becomes self-juxtaposed, providing a possible pathway for hydraulic connectivity (Fig. 9 inset, point 'A'). Adjacent to this, a westward-dipping NNW–SSE-striking fault is present on the flank of a salt-cored anticline. The anticline tightens to the south, increasing the dip on the flanks. The fault plane has been exploited by salt movement along the southern trace of the structure, where a salt wall and overhang have developed (Fig. 9, 'B'). Towards the southern end of the structure a second salt wall is developed to the west, forming parallel to 'B' (Fig. 9 inset, 'C'). The western salt wall increases in size over a short distance, having initiated as a

Downloaded from https://www.lyellcollection.org by UK Research and Innovation (UKRI/BGS/BAS) on Aug 13, 2025

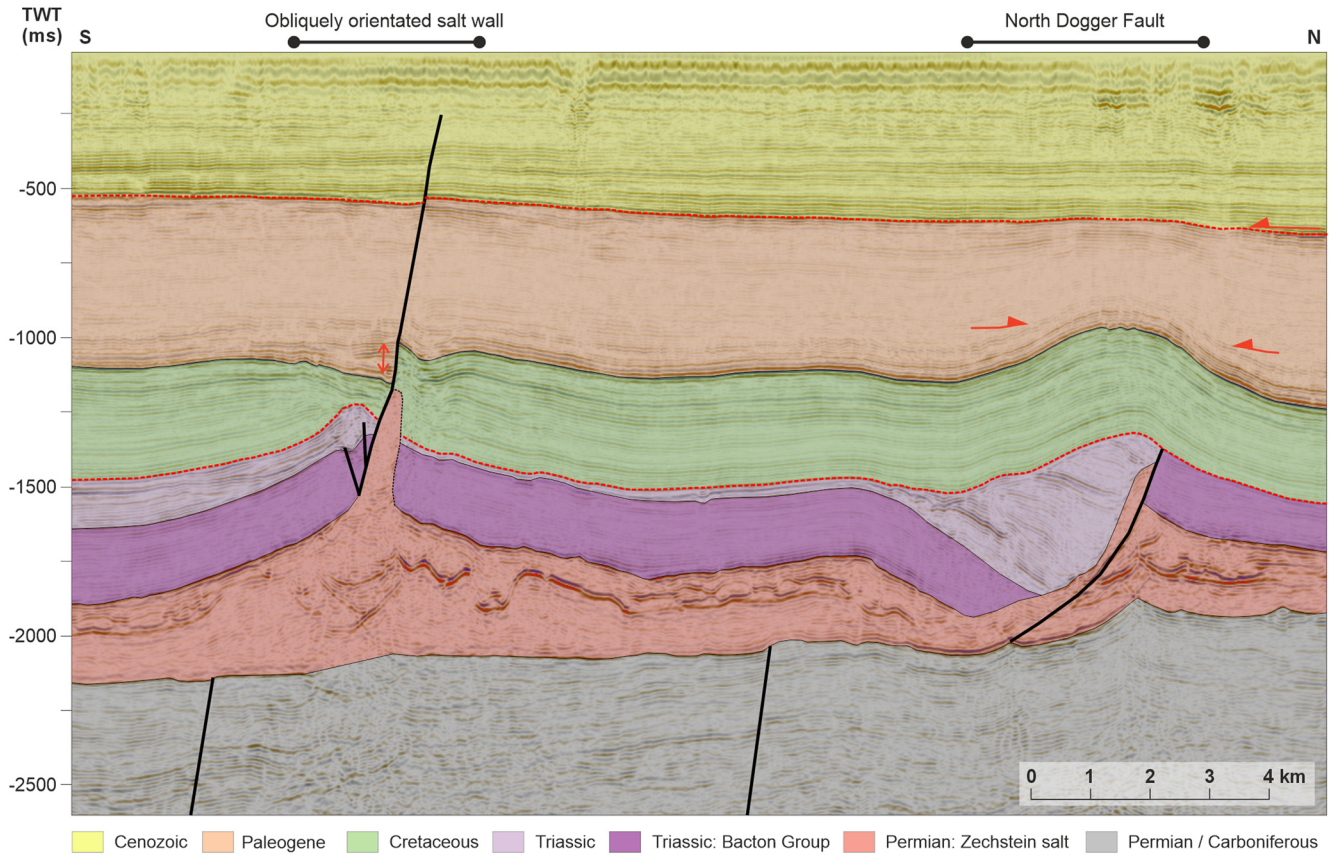

Fig. 7. Cross-section through the North Dogger Fault Zone. The southward-dipping North Dogger Fault terminates at the Base Cretaceous Unconformity. Later inversion during the Late Cretaceous to Paleogene resulted in folding above the fault. The salt wall to the south of the North Dogger Fault is obliquely orientated to the fault plane. Both structures divide the Bacton Group strata and provide lateral offset that probably inhibits pressure communication across the Bunter Sandstone Formation. The location of the section is shown in Figure 6. The red arrows denote stratigraphic features within the section (e.g. unconformities, syndeposition in the hanging wall of the fault and onlapping geometries on to the anticline). Source: contains information provided by the North Sea Transition Authority and/or other third parties.

reactive roller in the hanging wall of a fault (Fig. 9, 'D'). However, the geometry of the western salt wall is more open and broadens east–west, transitioning into a salt anticline with reduced deformation of the overburden, juxtaposing the Bacton Group. In contrast, separation of the Bacton Group is maintained across the eastern salt wall ('B').

This is a highly complex structural boundary resulting from multiple stages of development. Faulting probably initiated in the Late Triassic or Early Jurassic, as is observed across much of the UKSNS. This is indicated by the relatively uniform thickness of Lower Triassic sediments either side of the feature (Fig. 9). Jurassic strata are only preserved in localized areas owing to erosion beneath the BCU, which removed much of the Jurassic sediments (as well as Upper Triassic strata in some areas). Offset of reflections is observed at the level of the MMU, indicating that fault movement continued into the Neogene. Onlap is observed on the MMU with Neogene infill into faulted depocentres above the salt structures.

The boundary consists of multiple sections with different classifications (Fig. 4) along its length. In general, where the boundary is characterized by faulting, the faulting offsets the Bacton Group in the north (Class 5) and is typically self-juxtaposed (Class 2) in the south. Antithetic faults are usually present, with various configurations along the boundary, which might further impede connectivity across the East Silverpit Fault Zone. Detailed fault seal analysis studies are required to provide further information on potential flow behaviour. At point 'A' (Fig. 9), there is a clear communication pathway. However, the complexity of the intervening area between the two parallel salt walls, in combination with the proximity to the erosional boundary of the Bacton Group beneath the BCU, and the presence of Paleogene igneous dykes (Fig. 1), necessitates a dedicated interpretation study to resolve. In other segments of the boundary, mobile salts of the Zechstein Group have exploited the faults as zones of weakness, with development of reactive salt structures that clearly fully displace the Bacton Group strata (Class 6). Where these are fully developed as salt walls, the probability of communication across the structural boundary is low (Class 7). The complexity of the East Silverpit Fault Zone results in some uncertainty regarding the potential for hydraulic communication in the eastern part of the Silverpit Basin and the wider region.

Outer Silverpit Fault Zone

The Outer Silverpit Fault Zone is a salt-dominated, E–W-striking structure that separates the Silverpit Basin to the north and the Sole Pit High to the south (Glennie and Boegner 1981). Along the boundary length, the Bacton Group is separated either by salt intrusion (Fig. 10a) or a salt-dominated graben (Figs 10b, c, 11), with salt utilizing fault planes for migration and uplifting the post-salt strata. In the west, salt walls dominate and divide much of the post-Zechstein succession. In the east, salt domes and anticlines are present, and the boundary comprises a graben with allochthonous salt wings intruding into the Röt Halite. The transition between end member geometries takes place gradually along the length of the structure (Fig. 10).

The Zechstein evaporites detach the Mesozoic and Cenozoic post-Zechstein cover rocks from older Carboniferous and Permian strata, resulting in different structural configurations in the supra-salt strata. There is an additional detachment at the level of the Röt

Downloaded from https://www.lyellcollection.org by UK Research and Innovation (UKRI/BGS/BAS) on Aug 13, 2025

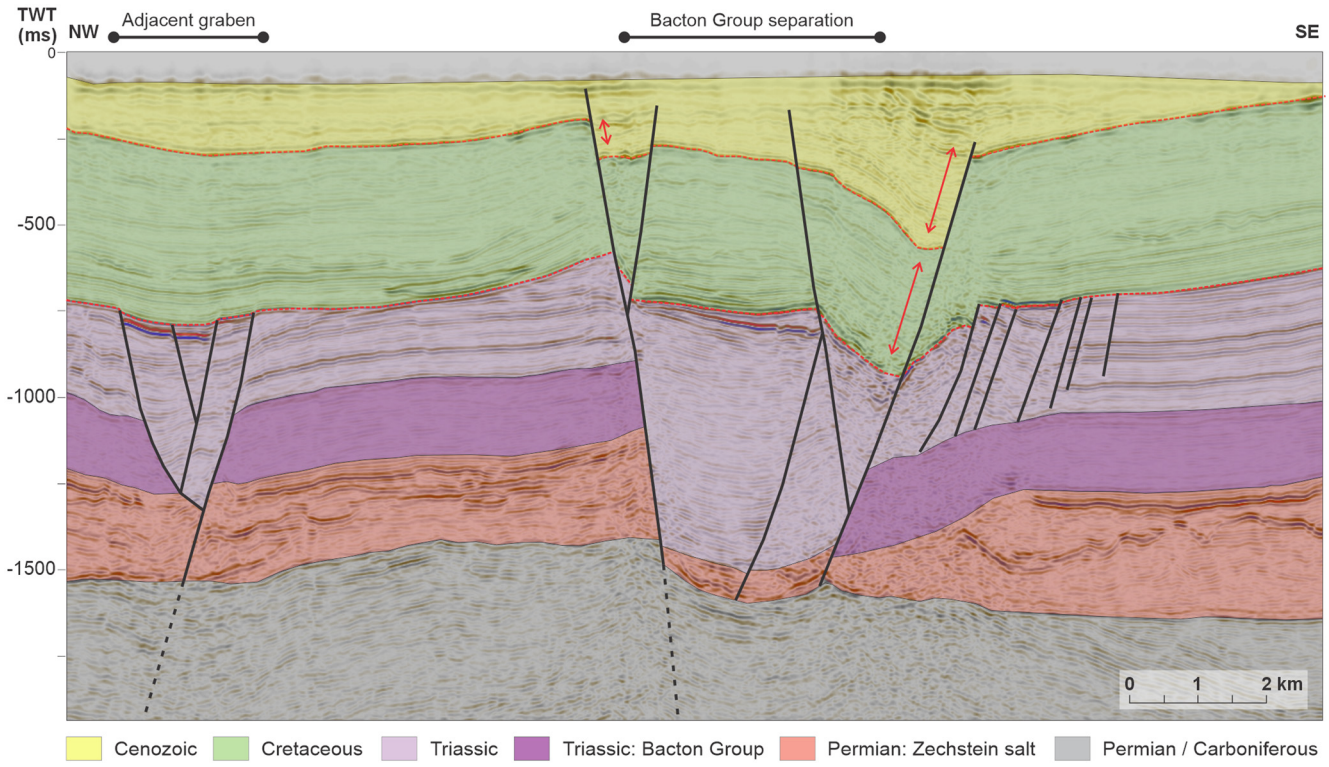

Fig. 8. Cross-section through the western section of the North Dogger Fault Zone. This transtensional graben system resembles the geometry of the Dowsing Graben System. Extension along this margin accommodates the shortening in the centre of the UK Southern North Sea. The geometry of the graben changes laterally and the SE–NW-dipping fault becomes more dominant, where it extends vertically, offsetting the shallower Neogene-aged strata above. Within the graben, the Bacton Group is predominantly absent, providing a clear zone of separation between Bacton Group strata in adjacent areas; salt intrusion is interpreted along some sections of the fault. Source: contains information provided by the North Sea Transition Authority and/or other third parties.

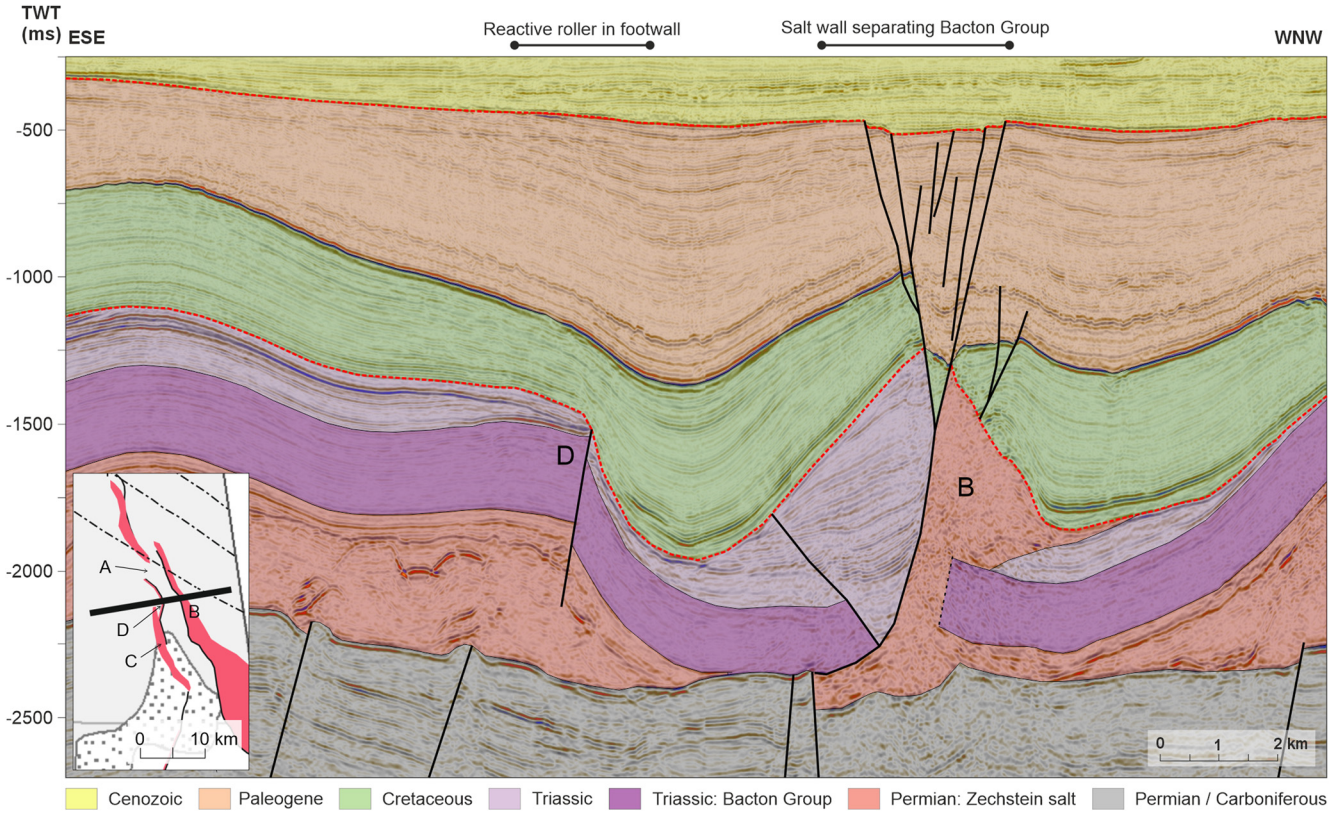

Fig. 9. Salt-dominated boundary along the East Silverpit Fault Zone. The complexity of the boundary is illustrated in this section. The juxtaposition of the Bacton Group at 'D' provides a potential pathway for fluid migration and therefore pressure communication. However, the faulting and salt intrusion at 'B' will probably inhibit hydraulic communication across the structure. The inset map shows that (out of the section plane) there are possible pathways northwards into the area east of the East Silverpit Fault Zone, and southwards to the erosional margin of the Bunter Sandstone Formation. Source: contains information provided by the North Sea Transition Authority and/or other third parties.

Downloaded from https://www.lyellcollection.org by UK Research and Innovation (UKRI/BGS/BAS) on Aug 13, 2025

Halite, which prevents faults that were formed by folding of the post-Zechstein strata from penetrating downwards into the BSF. The Röt Halite is prone to invasion by mobile Zechstein salt, resulting in the development of large allochthonous salt bodies (Fig. 11). These two detachments effectively isolate the Bacton Group, which acts as a relatively undeformed ridged beam.

Extensional faulting on the Outer Silverpit Fault commenced following deposition of the Bacton Group and Upper Triassic strata, which have consistent thicknesses in the vicinity of the structure (Fig. 11). Mobilization of the Zechstein salt and the resulting salt anticlines uplifted the Triassic sediments. Within the Bacton Group, brittle deformation is concentrated along the Outer Silverpit Fault

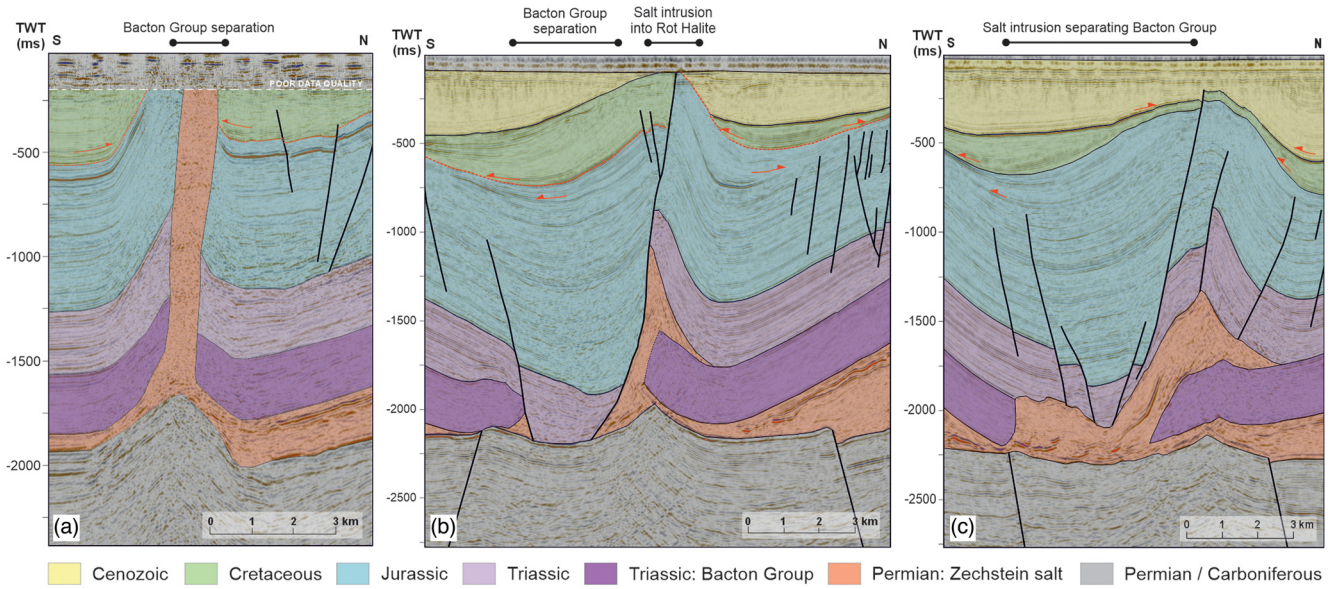

Fig. 10. Cross-sections transecting the Outer Silverpit Fault Zone. (**a**) Salt diapir bisecting the Bacton Group. (**b**) Salt utilizing the bounding faults of the graben as a migration pathway. (**c**) Salt-dominated graben. The location of each section is shown in Figure 6. The red arrows denote onlapping geometries of the seismic reflectors and the red dashed line represents the Base Cretaceous Unconformity. These sections show the range of structural styles observed along the boundary length. In each section, the Bacton Group strata are completely separated by the intervening salt walls, forming zones where no pressure communication is expected within the Bunter Sandstone Formation aquifer. Source: contains information provided by the North Sea Transition Authority and/or other third parties.

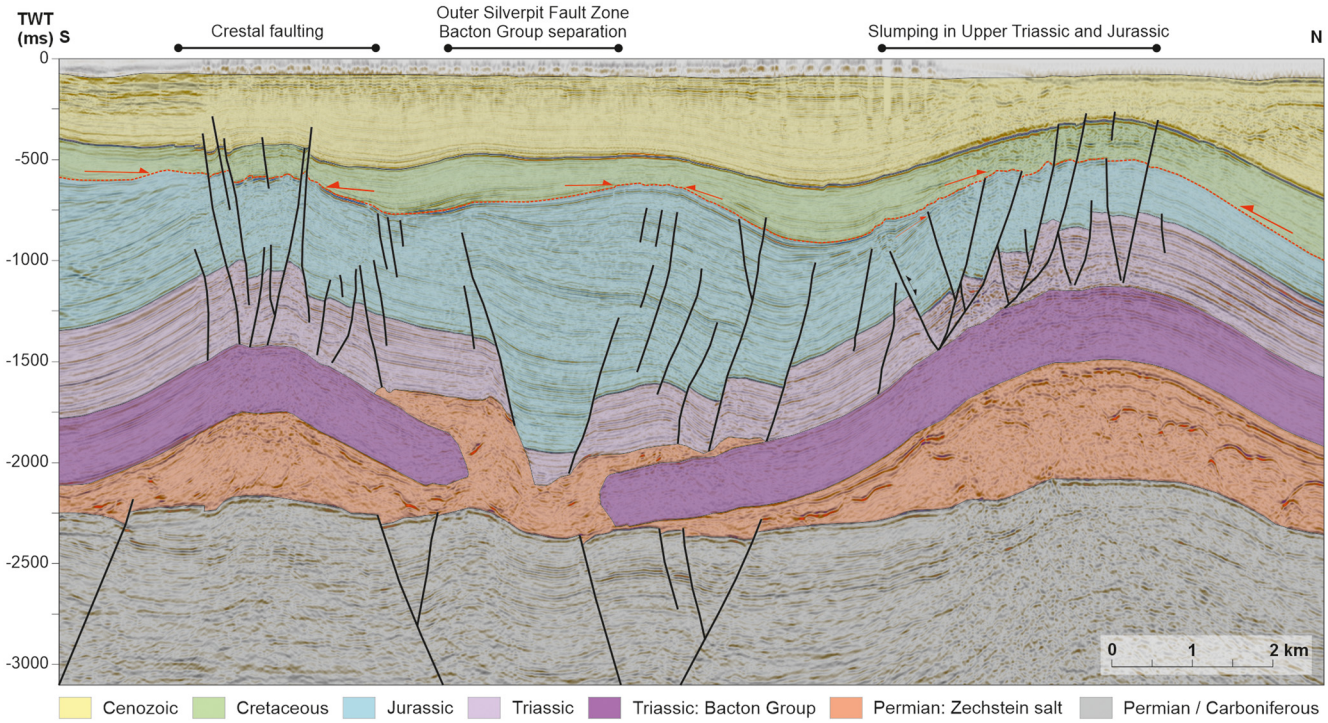

Fig. 11. Cross-section transecting the Outer Silverpit Fault Zone. The location of the section is shown in Figure 6. The red arrows denote onlapping geometries of the seismic reflectors and the red dashed line represents the Base Cretaceous Unconformity. The main faults forming the graben acted as a conduit for migration of the Zechstein salt. The Röt Halite, which is situated above the Bacton Group, acts as a detachment for deformation in the strata above and isolating the Bacton. The Zechstein salt utilized this plane of weakness along the mid-Triassic Röt Halite, intruding into it to form salt wings. There is significant lateral separation of the Bacton Group strata across the Outer Silverpit Fault, and consequently no pressure communication within the Bacton Group aquifer is expected across the boundary. Source: contains information provided by the North Sea Transition Authority and/or other third parties.

Downloaded from https://www.lyellcollection.org by UK Research and Innovation (UKRI/BGS/BAS) on Aug 13, 2025

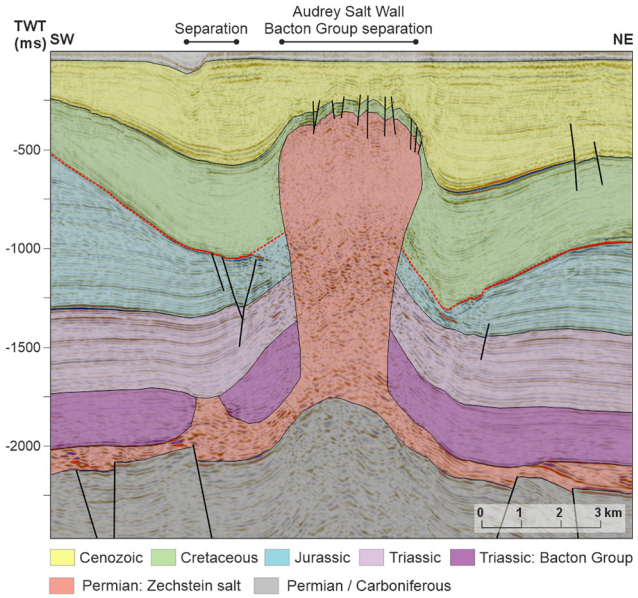

Fig. 12. Cross-section through the Audrey Salt Wall. This regionally extensive salt wall divides the Sole Pit High from the Inde Shelf to the east. It bisects the Triassic and Jurassic strata completely, separating the Bacton Group strata on either side of the structure. The zone of separation is up to 5 km wide, which likely provides a substantial barrier to fluid migration. Source: contains information provided by the North Sea Transition Authority and/or other third parties.

Zone, with little evidence of faulting at the crests of the anticlines, with extension largely accommodated in the overburden. Thickening of Jurassic strata is observed in the central graben of the Outer Silverpit Fault Zone (Fig. 10), and displacement and folding of the overlying Cretaceous and Cenozoic imply that salt movement continued during these periods. The timing of the intrusion of the Zechstein salt into the Röt Halite is difficult to determine, but there is some indication in Figure 10c that this may have occurred contemporaneously with the continued movement of the Zechstein salt during the Mid to Late Jurassic, as evidenced by onlapping geometries on to the anticline and the constant thickness of earlier Jurassic strata observed within the hanging wall (although this is not universally observed).

Across the structure, the Bacton Group is separated by a 2–3 km zone of mobile Zechstein evaporites (Fig. 11), and there is a low probability of potential pressure communication across the Outer Silverpit Fault Zone. The Outer Silver Pit Fault Zone is categorized as a Class 6 or 7 structural boundary, depending on the dominance of the faulting (e.g. the salt intrusion in Figure 10 defines the style of separation, while in Figure 10b, c the separation of the Bacton Group is defined by an interplay of both salt intrusion and faulting).

Audrey Salt Wall

The Audrey Salt Wall (Allsop *et al.* 2023) is orientated NNW–SSE and divides the Sole Pit High from the Inde Shelf to the east (Fig. 1). This regionally extensive salt wall is *c.* 40 km in length and up to 5 km wide. Brennan and Adam (2023) identified the onset of salt mobilization at the Audrey Salt Wall during the Triassic, with activity through the Jurassic and Cretaceous, but interpret cessation of movement during the Paleogene. In cross-section the Triassic and Jurassic strata are approximately uniform in thickness, with parallel bedding and little deformation evident away from the intrusive structure. In some areas along the Audrey Salt Wall, normal faulting is observed in the Triassic and Jurassic sediments on its flanks. Here it is interpreted that breakthrough commenced during a period of erosion resulting from Cimmerian uplift, which acted to reduce the overburden thickness, thereby enabling the breakthrough of mobile salts during the Cretaceous. Movement on the normal faults on the flanks of the salt wall continued during the Cretaceous, which is evidenced by thickening of strata in the hanging wall. Onlapping of the Cenozoic-aged strata on to the salt wall, and thickening of the strata towards it, suggest continued salt movement during the Cenozoic.

The Audrey Salt Wall separates the Bacton Group by up to 5 km and completely bisects Triassic, Jurassic and Cretaceous strata (Fig. 12), and as such the boundary is categorized as Class 7; aquifer communication across this structure is therefore unlikely.

Audrey Graben

At the southern end of the Audrey Salt Wall there is a transition from the salt-dominated structure to a NW–SE graben, termed here the Audrey Graben (Fig. 13a). To the south of the Audrey Salt Wall, this boundary separates the Sole Pit High to the west from the Inde Shelf to the east. Significant auxiliary faulting is observed along the flanks; however, this is mostly limited to the strata above the Bacton Group, with faults soling out in the Röt Halite. There is little difference in the stratigraphic thickness of the Triassic sediments, which otherwise display parallel and continuous seismic reflectors/seismic facies. By contrast, there is substantial thickness variation within the Jurassic-aged strata. Erosion beneath the BCU accounts for this variation in the Jurassic; there is little evidence of onlapping reflections and the bedding is broadly parallel with the underlying Triassic sediments (Fig. 13a). Rifting along the Audrey Graben probably initiated during the Jurassic and continued through the Cretaceous and into the Paleogene. There is substantial thickness variation in Cretaceous-aged strata, with onlapping of reflections observed on to the eroded BCU surface. Wedge-shaped geometries in the Paleogene indicate syndeposition representing a further period of movement.

The configuration of bounding faults shown in Figure 13b suggests a lateral component to movement on these faults. A central horst is bounded by two graben and internal faulting. There is generally complete separation of the Bacton Group strata across the structural boundary, with large offsets observed across the main bounding faults (Class 5). It is possible that some juxtaposition may be present locally. The boundary is complex with many intersecting faults, and a more detailed interpretation would be required to properly assess juxtaposition.

Mid Sole Pit Fault

The name Mid Sole Pit Fault is given to the structure that both bisects the Sole Pit High and connects the Audrey Graben with the Dowsing Graben System. The E–W-striking feature is not marked on many older structural maps of the basin but is shown in the structural maps of Doornenbal and Stevenson (2010). Recent publications on salt tectonics and salt structure morphologies in the UKSNS identify the presence of salt structures within this lineament (Brennan and Adam 2023; Brennan *et al.* 2023). This structure likely developed as a transfer fault in response to regional stresses, with salt utilizing the plane of weakness during mobilization. The salt structure is characterized as a reactive diapir by Brennan *et al.* (2023).

Where the Mid Sole Pit Fault intersects with the Dowsing Graben System, a graben completely displaces the Bacton Group. This part of the structure is categorized as a Class 5 structural boundary. Mobile salt is present along much of the boundary and a narrow salt wall separates the Lower Triassic strata in the west, resulting in a Class 7 categorization. In some sections, the salt does not appear to completely intrude into the Bacton Group, with some connection remaining above the diapir (Class 4; Fig. 5d). A larger southward-dipping fault is present at the midpoint of the boundary, which extends into the overlying Jurassic strata and possibly up to the

Downloaded from https://www.lyellcollection.org by UK Research and Innovation (UKRI/BGS/BAS) on Aug 13, 2025

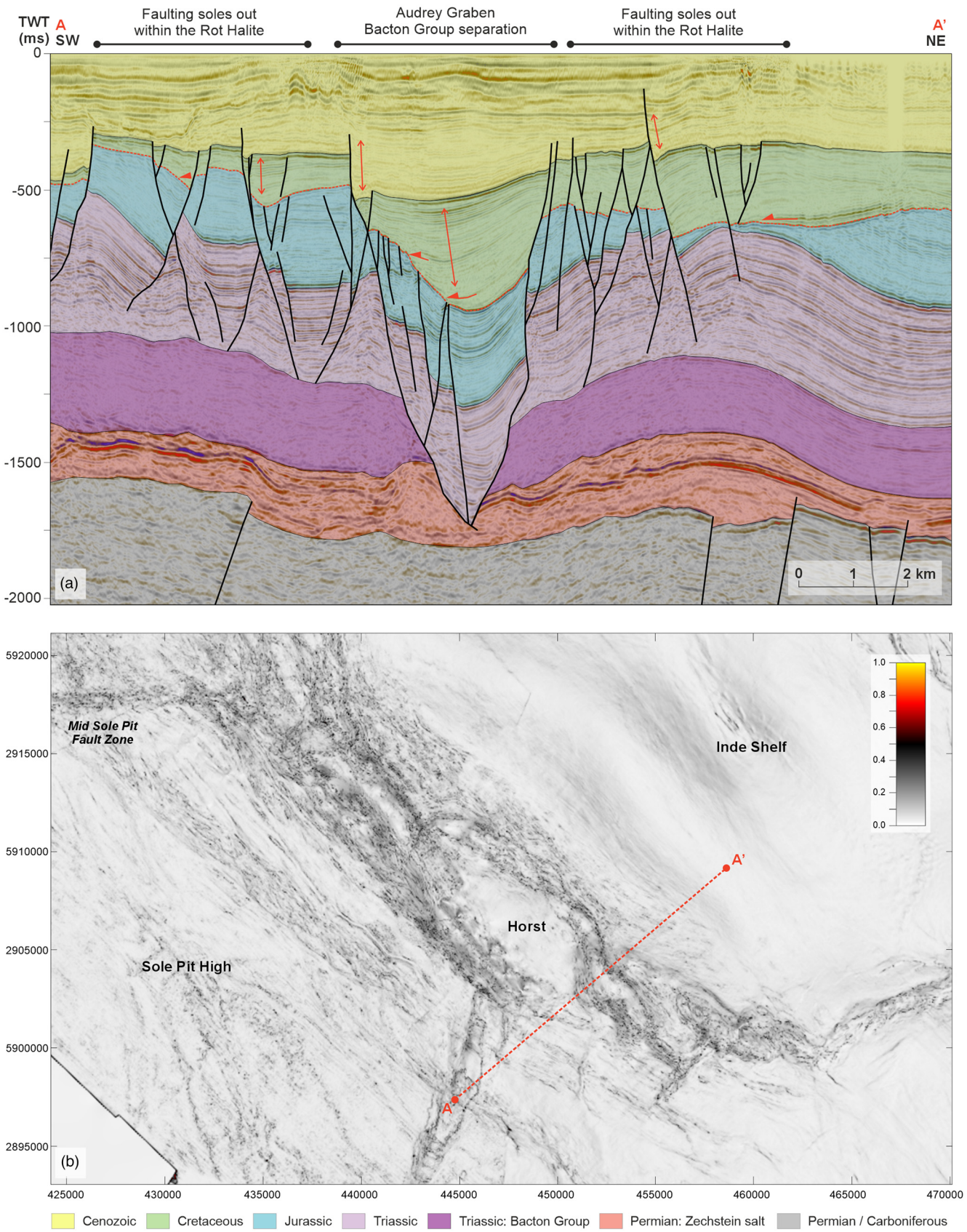

Fig. 13. Audrey Graben. (**a**) Cross-section through the Audrey Graben; the location of the section is shown in Figure 6 and (b). (**b**) Structurally smoothed variance map of the top Bacton surface showing the Audrey Graben. The profile A–A′ marks the location of (a). The NE–SW graben separates the Sole Pit High from the Inde Shelf. Complete separation of the Bacton Group strata, as well as large offsets across the bounding faults, is likely to inhibit pressure communication within the Bunter Saline Aquifer. Significant auxiliary faulting is observed adjacent to the main graben; however, this is mostly limited to the strata above the Bacton Group, with faults soling out in the Röt Halite. The red arrows denote stratigraphic features within the section (e.g. unconformities, syndeposition in the hanging wall of the fault and onlapping geometries on to the anticline). Source: contains information provided by the North Sea Transition Authority and/or other third parties.

Downloaded from https://www.lyellcollection.org by UK Research and Innovation (UKRI/BGS/BAS) on Aug 13, 2025

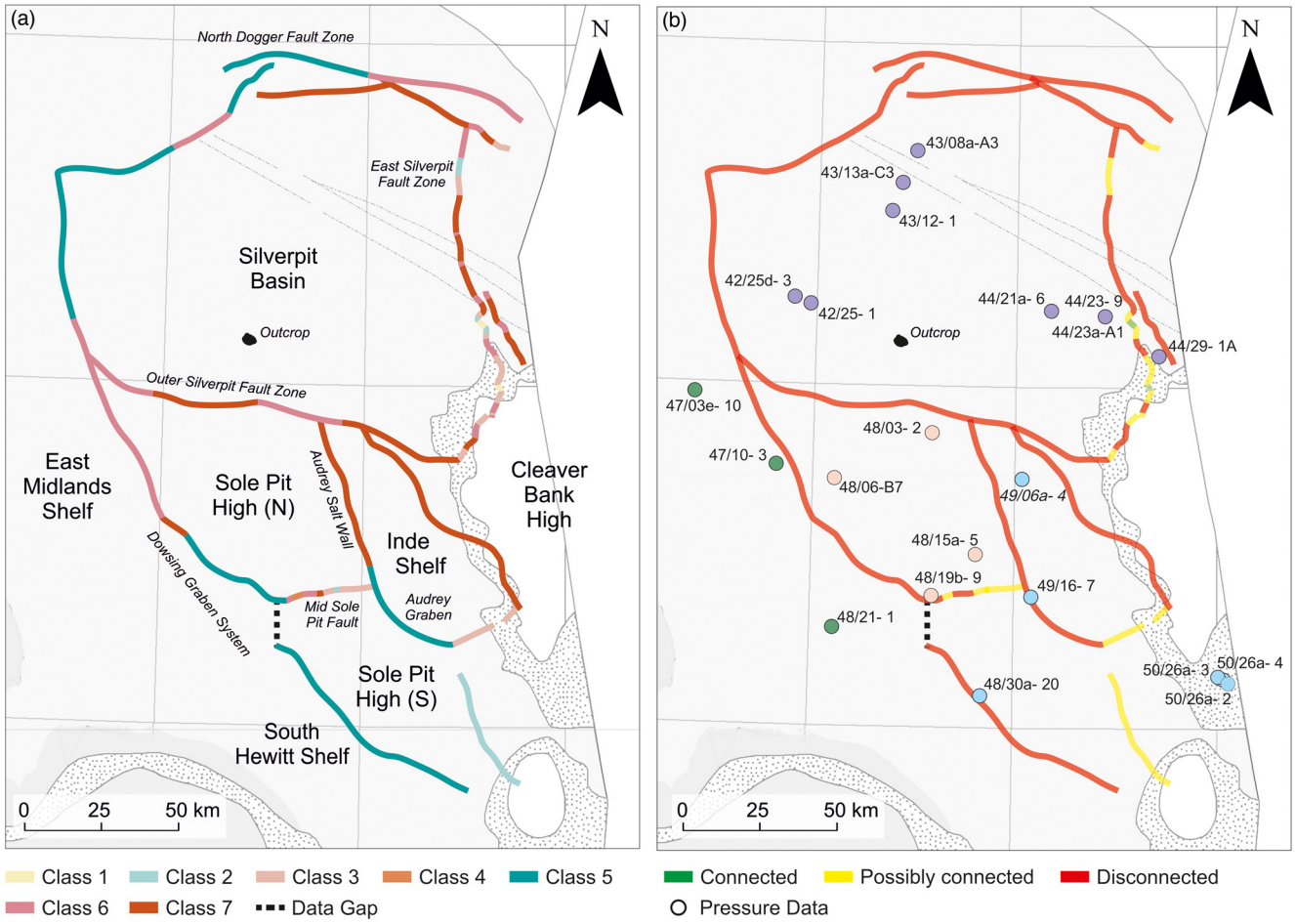

Fig. 14. Boundary classification maps. (**a**) Classification according to the geometric relationship of the Bacton Group across the structure. (**b**) Degree of likely connectivity across the boundaries including the mapped pressure data. Well datapoint colours correspond with those shown in Figure 15. Source: contains information provided by the North Sea Transition Authority and/or other third parties.

seabed. Here, salt utilizes the fault plane to form a reactive salt diapir (Class 6; Fig. 5c). The vertical offset decreases to the east, where the single southerly dipping fault no longer displaces the overburden. The offset of the Bacton Group strata is generally low, but variable along the structure, which is partly accommodated by thickening of the Zechstein salt in the east.

There is a reduction in seismic quality along the eastern section of the boundary, and as a result it becomes more difficult to interpret the boundary. Small offsets of Bacton Group strata, and a general chaotic reflectivity in this part of the dataset, result in this part of the boundary being categorized as Class 3.

There is more uncertainty associated with the interpretation of this boundary. Detailed seismic interpretation is required to learn more about this largely undocumented structure to learn more about both the deformation history and the geometry of the structure. This would enable more insight into the likelihood of pressure communication across the boundary. It is, however, clear that brittle deformation within the Bacton Group is concentrated along the Mid Sole Pit Fault. The deformation style changes significantly above the Röt Halite. This deformation is particularly concentrated around a NW–SE-striking feature located in the centre of the Sole Pit High. Here, post-Triassic strata are heavily faulted; however, the faults detach within the Röt Halite and do not make a significant impact on the hydraulic unit.

Summary of boundary conditions

The structural boundaries described above have been categorized to determine the degree of connectivity across the BSF. The resulting boundary condition map is shown in Figure 14. The map shown in Figure 14b strongly suggests that the BSF in the UKSNS can be subdivided into several distinct hydraulic units. The main units correspond to the Silverpit Basin, Sole Pit High and the Inde Shelf, with potential for further subdivision such as the distinction between the northern and southern parts of the Sole Pit High. As illustrated in Figure 14, the BSF appears to be disconnected across the Dowsing Graben System, separating the central part of the basin from the East Midlands Shelf and Cleveland Basin to the west. In this study, the potential connection between the East Midlands Shelf and Cleveland Basin was not evaluated but is recommended as the subject of further work.

Silverpit Basin

The large zones of separation between the BSF within the Dowsing Graben System strongly suggest that pressure communication is not anticipated between the Silverpit Basin and the Cleveland Basin to the west. The Outer Silverpit Fault Zone also laterally disconnects the Bacton Group due either to salt walls or a *c*. 3.5 km wide graben bound by allochthonous salt intrusions into the Röt Halite. Consequently, the Silverpit Basin is expected to behave as a distinct hydraulic unit during CO_2 injection.

Based on the structural interpretation presented, the potential for pressure communication across the East Silverpit Fault Zone into the eastward extension of the Silverpit Basin is less clear. There is a high degree of structural variation and there is potential for connection of the BSF aquifer across sections of the boundary (Fig. 14). Fault seal analysis studies will be required to evaluate the

Downloaded from https://www.lyellcollection.org by UK Research and Innovation (UKRI/BGS/BAS) on Aug 13, 2025

potential for pressure communication across the East Silverpit Fault Zone.

Sole Pit High

Bound by the Dowsing Graben System, Outer Silverpit Fault Zone and the Audrey Salt Wall on the western, northern and eastern boundaries, respectively, the northern part of the Sole Pit High is likely to behave as a closed hydraulic unit. The Mid Sole Pit Fault Zone is expected to inhibit communication with the southern part of the Sole Pit High in its western extension, either through complete displacement of the Bacton Group strata by faulting or disconnection by salt intrusion. At the eastern extent of the Mid Sole Pit Fault Zone there is less fault displacement, together with a reduced presence of reactive salt structures. Seismic data quality is also reduced owing to a highly deformed overburden, which introduces more uncertainty from a structural perspective. Consequently, the BSF is considered to be possibly connected across parts of the boundary between the northern and southern parts of the Sole Pit High.

To the south of the Mid Sole Pit Fault Zone, the eastern boundary of the Sole Pit High is defined by faulting. These faults are categorized as either Class 2 or 5. There is complete displacement of the Bacton Group along the Audrey Graben that limits the likelihood for pressure communication between the Sole Pit High and the Inde Shelf to the east. South of the Audrey Graben fault displacement reduces, juxtaposing the Bacton Group.

Further, there is an increase in the frequency of faults towards the southeastern margin of the Sole Pit High (Fig. 1). Thinning of the Zechstein evaporites in this area results in a change in deformation style, from thin to thick skinned, with increased soft and hard linking of faults into the basement. It is possible that sub-seismic scale faults are present to the south of the Audrey Graben; however, the displacements would be low, reducing the likelihood that the BSF is entirely disconnected, and therefore pressure communication may occur. The structural complexity in this region merits further studies involving detailed mapping of the structures and assessment of the potential for self-juxtaposition of the BSF.

Inde Shelf

The Inde Shelf to the east of the Sole Pit High is bound predominantly by salt walls on the northeastern and western margins (Audrey Salt Wall), faulting on the southwestern margin (Audrey Graben) and faulting with the influence of salt on the southern margin. These structures provide confidence that pressure communication with the adjacent hydraulic units is unlikely. The SW–NE-orientated faults that cut across the Inde Shelf to the SE of the Audrey Graben have little to no vertical displacement and are likely to have a strike-slip component to displacement. As with the other SW–NE-orientated boundaries, such as the Mid Sole Pit Fault Zone, minor salt intrusion occurs along faults. Consequently, these features are categorized as possibly connected (Fig. 14), and further work is required to characterize the fault characteristics and their likely impact on pressure communication within the Inde Shelf.

Validation of results

The interpretation presented in Figure 14 is supported by compilation of regional pressure data from the BSF in the UKSNS. The pressure data indicate that there are distinct pressure regimes in the different structural regions identified above (Fig. 15). These pressure regimes are observed in the Silverpit Basin, the northern part of the Sole Pit High, the Inde Shelf and southern part of the Sole Pit High, and along the margins of the East Midlands Shelf and in the Dowsing Graben System. The data plotted in Figure 15 have been colour-shaded to reflect the different parts of the basin in which the wells are located. While there are relatively few pressure data available from the BSF, Figures 14b and 15 provide compelling evidence to support the structural interpretations described above. This strongly suggests that the structures highlighted in Figure 14 have compartmentalized the distinct hydraulic units over geological timescales.

Silverpit Basin

The pressure regime in the Silverpit Basin is notably different from that in the Sole Pit High to the south (Fig. 15). This supports the lack of aquifer connectivity inferred from the seismic interpretation across the Outer Silverpit Fault Zone. There is some uncertainty along parts of the eastern extent of the basin where the Bacton Group is disconnected across the East Silverpit Fault Zone. This may imply a further hydraulic unit east of the fault zone, although juxtaposition is interpreted along some sections of the structure. Additionally, the BSF in well 44/29-1A shares a common pressure regime with the wells to the west of the structure (Fig. 14b); however, evidence for hydraulic connectivity (or otherwise) across the structure remains limited. The data shown on Figure 14b also suggest that similar pressure regimes prevail on either side of the Paleogene igneous dyke features across the Silverpit Basin area. At least on geological time frames, the dykes do not appear to compartmentalize the BSF (Bentham *et al.* 2017), although uncertainty remains.

Sole Pit High and Inde Shelf

The elevated pressure regime observed in the northern part of the Sole Pit High is likely to have resulted from basin inversion. The data confirm that the southern part of the Sole Pit High is hydraulically isolated from the northern part, with a more normal pressure regime in the south. The southern part of the Sole Pit High, to the south of the Audrey Salt Wall, may be in communication with the Inde Shelf to the east where there are possibly connected boundary features, and the structural interpretation is more uncertain. It is worth noting that there is a lack of direct pressure measurement data with which to constrain the pressure regimes across the southern part of the Sole Pit High and both the northern and southern extents of the Inde Shelf.

East Midlands Shelf and Dowsing Graben System

The wells that have significantly higher observed pressures, along the western margin of the Dowsing Graben System, lie beyond the extent of the seismic data available. These high pressures may result from localized compartmentalization, with laterally isolated BSF preserved on horst structures within the Dowsing Graben. Some of these isolated incidences of BSF may have been subject to inversion during Cretaceous or Cenozoic inversion events (Fig. 2). The data probably do not provide an indication of the BSF pressure regime prevailing on the East Midlands Shelf, which is difficult to constrain owing to lack of data. However, the higher-pressure measurements along the axis of the Dowsing Graben System support the notion that this major structural boundary acts to isolate the hydraulic units to the east and west.

Discussion

Connectivity within the Bunter Sandstone Formation

This study has shown that the BSF of the UKSNS can be subdivided into several large hydraulic units, separated by major fault zones and salt structures that have been influenced by halokinesis. With some exceptions, the Bacton Group is likely to be disconnected across these intervening structural boundaries such that pressure communication between the compartments is unlikely. The study has

Downloaded from https://www.lyellcollection.org by UK Research and Innovation (UKRI/BGS/BAS) on Aug 13, 2025

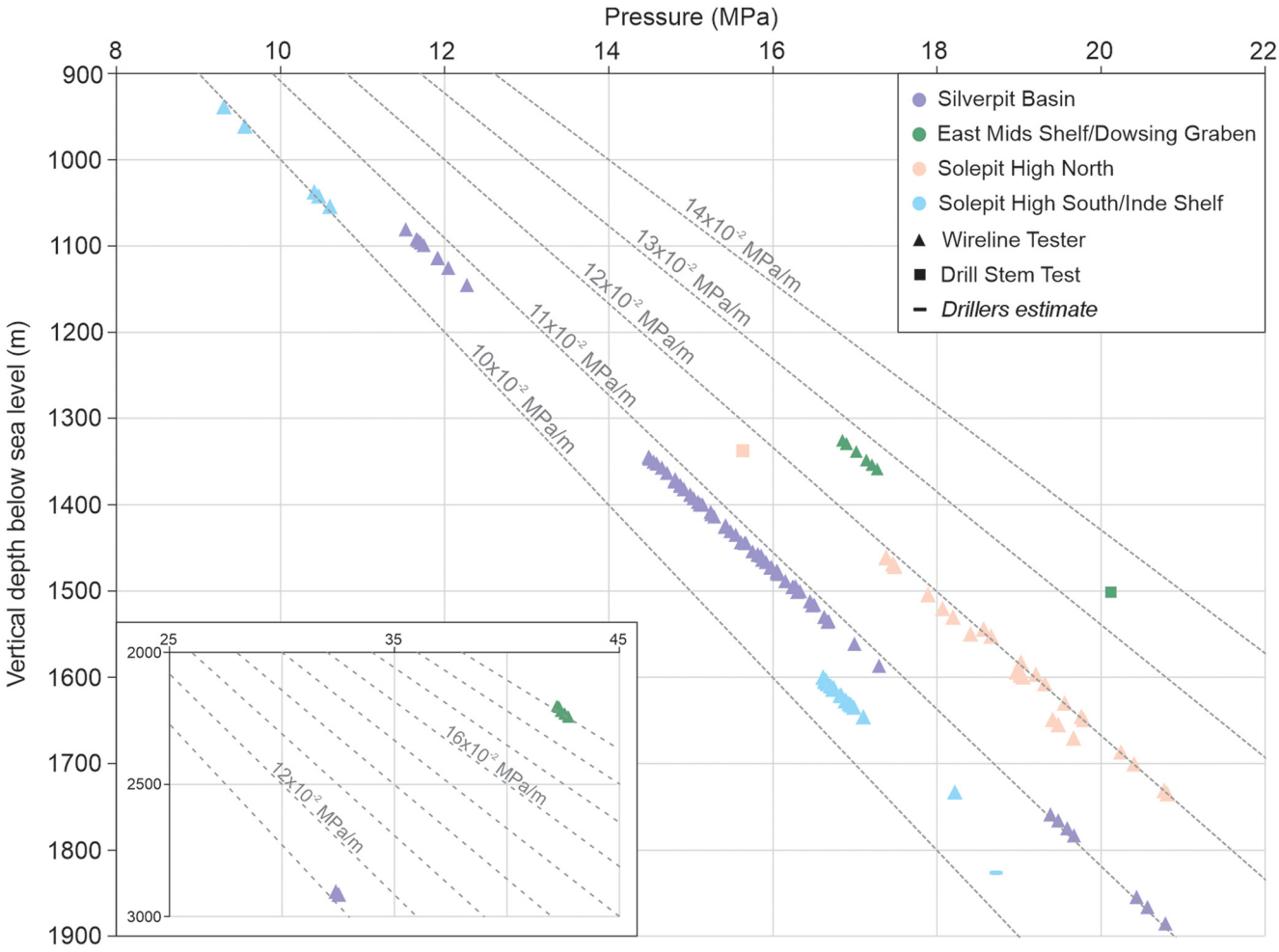

Fig. 15. Pressure–depth plot. The inset is included to show the values at the extreme pressure and depth range. Note that the driller's estimate reported for well 49/06a-4 (see location in Fig. 14) does not represent a true pressure measurement.

focused on the central part of the basin to the east of the Dowsing Graben System, where the main compartments include the Silverpit Basin, the northern and southern sections of the Sole Pit High, and the Inde Shelf. However, the study does not preclude the possibility that other, smaller compartments are also present.

Pressure measurements support the structural interpretation, with clear pressure differentials between adjoining structural compartments. This is most clearly illustrated by the distinct pressure regime in the Silverpit Basin, relative to higher overpressures in the northern part of the Sole Pit High, and lower gradients in the south of the Sole Pit High and eastwards on to the Inde Shelf (Fig. 15). Previous studies in the Silverpit Basin region (i.e. Noy *et al.* 2012; Bentham *et al.* 2017) assumed that the structures surrounding the sub-basin would isolate the aquifer from the surrounding region and that there are few, if any, internal barriers to flow within it. The analysis of pressure data presented here supports the notion that separate CO_2 storage licences within the Silverpit Basin are likely to share a common saline aquifer. As such, it is likely that operations within the region will impact on one another. Conversely, CO_2 storage operations in the BSF located either side of the Dowsing Graben System, Outer Silverpit Fault Zone and Audrey Salt Wall are unlikely to exhibit hydraulic communication owing to the clear spatial dislocation of the aquifer across these major structural boundaries. With a comparable pressure regime in both the southern part of the Sole Pit High and the Inde Shelf and southern margins of the Cleaver Bank High, some uncertainty remains around the potential for pressure communication across the Audrey Graben and particularly across the faults south of the graben.

Boundary classification scheme

The new classification scheme and methodology presented allows for a simplified classification of major structures and their possible impact on saline aquifer connectivity. While many of the structural boundaries can readily be categorized, structural complexities and limited data resolution can lead to uncertainty in categorization of others. In places, this study has encountered low signal to noise ratio, migration artefacts associated with the flanks of the anticlines and limited 3D seismic data along the North Dogger Fault Zone, which all may impact the certainty of classification. This uncertainty can be accounted for in the scheme by moving the classification up the tiers of the tertiary diagram; for example, Class 5 becomes Class 2, identifying it for further investigation.

By assessing the boundaries on the geometric relationships of the BSF, migration pathways up faults and into alternative aquifers are not accounted for. For some of the structural boundaries discussed here, a detailed evaluation of fault geometries and BSF juxtaposition is required to identify potential communication pathways across complex deformation zones. Additionally, the scheme is limited to structural boundaries and excludes stratigraphic features such as erosion or pinch out.

Beyond this study, as subsurface storage expands to other regionally extensive aquifers, the scheme has application for other regionally extensive aquifers with storage potential. It can be used to provide an assessment of pressure communication and offers a means to identify areas that require further investigation.

Downloaded from https://www.lyellcollection.org by UK Research and Innovation (UKRI/BGS/BAS) on Aug 13, 2025

Implications for CCS

Regional modelling studies have highlighted the potential for widespread pressurization of the BSF during CO_2 injection and storage (Noy *et al.* 2012; Agada *et al.* 2017). The apparent compartmentalization of the BSF in the UKSNS therefore has clear implications for the expected behaviour of the BSF saline aquifer in response to future CO_2 injection activities. Without active pressure management, for example through brine production (Pongtepupathum *et al.* 2017), it is possible that projects may induce pressure increases that negatively impact the pressure window available to other licences. Ultimately, this may result in a reduction of storage capacity.

It is worth noting that the risk of pressure communication across structural boundaries may have both positive and negative implications. The elevated pressure footprint from CO_2 injection is unlikely to extend beyond the structural boundaries identified, which may limit the likelihood of pressure communication between discrete CO_2 storage projects on opposing sides of one of the structures. Additionally, while smaller hydraulic units may be subject to rapid pressure build-up, the lateral extent of the elevated pressure response will be limited. Conversely, larger hydraulic units will facilitate wider distribution of excess pressure; a greater number of other subsurface users are likely to be impacted by the pressure response. In the case of the BSF in the UKSNS, the scale of the individual hydraulic units is such that considerable headroom is available.

Overpressurization of the aquifer will also have implications for any future drilling operations, which will need to account for the elevated pressure upon entering the BSF. Similarly, pressure connectivity across international boundaries is an important consideration owing to possible cross-border displacement of saline fluids (Hannis *et al.* 2013). While this issue is relevant to exploitation of the BSF, particularly in areas adjacent to the median line, it will also affect other potential saline aquifer storage sites in the North Sea.

The present study provides an understanding of the regions likely to be affected by early CO_2 storage projects while offering a framework for assessment of regional hydraulic unit connectivity. This understanding can be used as a foundation upon which CO_2 storage licence holders, regulatory agencies and governmental departments responsible for the UK's net zero targets can begin to evaluate the regional impact of storage operations in the BSF.

Wider implications

The extent to which CO_2 storage activities can affect aquifer pressure in the BSF saline aquifer is important for several other reasons. The displacement of highly saline pore fluids and the mobilization of heavy minerals presents an environmental concern. The BSF locally subcrops the seabed above a particularly high-relief salt diapir in the centre of the Silverpit Basin (Noy *et al.* 2012; Gluyas and Bagudu 2020); an increase in pore fluid pressure in the vicinity of the seabed subcrop could result in discharge of saline fluids to the seawater column (Noy *et al.* 2012). It is also uncertain if elevated pressure conditions could lead to the migration of saline pore fluids towards the surface via transmissive fracture zones, the reactivation of existing faults (Hannis *et al.* 2013; Williams *et al.* 2014) and/or through legacy wellbores.

Additionally, because the BSF rises towards the shoreline on the East Midlands Shelf. The displacement of saline pore fluids towards the UK coastline could result in encroachment of saline aquifer fluids in the direction of potable water resources. One further aspect of interest would be the potential geomechanical response to induced overpressure, which could have implications for regional seismicity and ground-surface heave, as observed at some active CO_2 storage sites (Verdon *et al.* 2013).

Conclusions

This study highlights key areas where pressurization of the BSF needs to be considered for the development of CO_2 storage in the UKSNS. Interpretation of seismic data was used to characterize the major structural features affecting the BSF, and to identify structural variations along-strike. A new classification scheme was developed to map this variation and to provide a framework to classify the likelihood of pressure communication across each boundary. In the UKSNS, it is expected that most of the boundaries evaluated will provide barriers, or at least significant baffles to flow, which will limit the extent of pressure communication across the structural boundaries. The Dowsing Graben System, Outer Silverpit Fault Zone, Audrey Salt Wall, Audrey Graben and North Dogger Fault Zone all provide significant separation of the BSF. These boundaries are therefore likely to separate the BSF into distinct hydraulic units. This finding has implications for the development of CO_2 storage in the BSF saline aquifer, particularly where multiple projects are intended to be developed within the same hydraulic unit.

Variation along the boundaries is captured by the classification scheme, providing detailed information on boundary conditions for numerical flow simulation models, including identification of areas where pressure communication may be possible across otherwise closed boundary structures. Areas of uncertainty remain where structures are highly complex, such as the southern portion of the East Silverpit Fault Zone. Features that contribute to increased uncertainty include areas where there is evidence of salt withdrawal along the boundary, transition zones between structures with variable deformation styles and at junctions between major structures. Application of the classification scheme enables the identification of areas where further characterization work may be required. For example, fault seal analysis on boundary sections where the BSF is offset by faulting would support an assessment of potential hydraulic connectivity across the faults. Additionally, regions where further detailed structural mapping may be required, to improve understanding of boundary conditions in zones of complexity, can readily be identified following application of the scheme.

The Silverpit Basin and the northern part of the Sole Pit High are areas where pressurization might be expected to be a key issue requiring consideration. Multiple carbon storage licences have been awarded in these areas and pressure data suggest that these structural regions are subject to distinct pressure gradients. This supports the expectation inferred from the seismic interpretation that there is no aquifer connectivity across the bounding structures, and suggests that they will act as isolated, albeit still very extensive, hydraulic units.

Although the classification scheme was developed to characterize the BSF in the UKSNS, the methodology can equally be applied to other regions where extensive saline aquifers are considered for CO_2 storage. The scheme enables a rapid appreciation of the extent of potential pressure impacts on a regional scale, providing vital information for regional simulation studies. This provides both an indication of connected pore volumes and the designation of appropriate boundary conditions for numerical simulation studies.

The development and management of saline aquifer storage sites will need to consider the potential for regional pressurization and impacts on available pressure budgets. This will be particularly pertinent where multiple CO_2 storage projects are exploiting saline aquifer targets located within the same hydraulic unit. Dynamic data, particularly those acquired during appraisal and development of CO_2 storage projects, will provide a key verification of the results presented here. A joint approach between relevant stakeholders, including operators, regulatory bodies and policymakers, will be required to facilitate timely distribution of such data. This would ensure that the storage capacity of extensive saline aquifers such as

Downloaded from https://www.lyellcollection.org by UK Research and Innovation (UKRI/BGS/BAS) on Aug 13, 2025

the BSF can be exploited safely and effectively, maximizing the available storage capacity in support of net zero targets.

Acknowledgements We acknowledge funding from the UK Carbon Capture and Storage Research Centre 2017 (EPSRC Grant EP/P026214/1) and the Industrial Decarbonisation Research and Innovation Centre (EPSRC Grant EP/V027050/1). The research also benefited from the Managing the Environmental Sustainability of the Offshore Energy Transition (MOET) project, funded by the NERC National Capability Multi-Centre Science programme.

Structural interpretation work was performed with support from the Research Council of Norway – FME NCCS Centre 257579/E20 and British Geological Survey National Capability funding from NERC.

Schlumberger are thanked for provision of the speculative seismic reflection data used for regional seismic mapping, and for provision of Petrel software licences used for seismic interpretation.

This paper is published with the permission of the Executive Director, British Geological Survey (NERC, UKRI).

Author contributions **LEA**: conceptualization (equal), data curation (equal), formal analysis (lead), investigation (equal), methodology (lead), writing – original draft (lead), writing – review & editing (equal); **JDOW**: conceptualization (equal), data curation (equal), formal analysis (supporting), funding acquisition (equal), investigation (equal), methodology (equal), writing – original draft (equal), writing – review & editing (equal); **KAW**: data curation (equal), investigation (equal), writing – original draft (supporting), writing – review & editing (equal); **TAR**: data curation (equal), investigation (equal), writing – review & editing (equal); **PB**: data curation (equal), investigation (equal), writing – review & editing (equal); **HAM**: data curation (equal), investigation (equal), writing – review & editing (equal); **TJHD**: data curation (equal), investigation (equal), methodology (supporting), writing – review & editing (equal); **GEP**: data curation (equal), investigation (equal), writing – review & editing (equal); **JCW**: funding acquisition (equal), investigation (equal), writing – original draft (supporting), writing – review & editing (equal)

Funding This work was funded by the Natural Environment Research Council (NE/W005026/1), Engineering and Physical Sciences Research Council (EP/P026214/1), Engineering and Physical Sciences Research Council (EP/V027050/1) and Norges Forskningsråd (257579/E20).

Competing interests The authors declare that they have no known competing financial interests or personal relationships that could have appeared to influence the work reported in this paper.

Data availability Data sharing is not applicable to this article as no datasets were generated or analysed during the current study.

References

Agada, S., Jackson, S. *et al.* 2017. The impact of energy systems demands on pressure limited CO_2 storage in the Bunter Sandstone of the UK Southern North Sea. *International Journal of Greenhouse Gas Control*, **65**, 128–136, https://doi.org/10.1016/j.ijggc.2017.08.014

Allen, M.R., Griffiths, P.A., Craig, J., Fitches, W.R. and Whittington, R.J. 1994. Halokinetic initiation of Mesozoic tectonics in the southern North Sea: a regional model. *Geological Magazine*, **131**, 559–561, https://doi.org/10.1017/S0016756800012164

Allsop, C., Yfantis, G., Passaris, E. and Edlmann, K. 2023. Utilizing publicly available datasets for identifying offshore salt strata and developing salt caverns for hydrogen storage. *Geological Society, London, Special Publications*, **528**, 139–169, https://doi.org/10.1144/SP528-2022-82

Bentham, M., Mallows, T., Lowndes, J. and Green, A. 2014. CO_2 STORage Evaluation Database (CO_2 Stored). The UK's online storage atlas. *Energy Procedia*, **63**, 5103–5113, https://doi.org/10.1016/j.egypro.2014.11.540

Bentham, M., Williams, G., Vosper, H., Chadwick, A., Williams, J. and Kirk, K. 2017. Using pressure recovery at a depleted gas field to understand saline aquifer connectivity. *Energy Procedia*, **114**, 2906–2920, https://doi.org/10.1016/j.egypro.2017.03.1418

Brennan, C. and Adam, J. 2023. Regional variability of onset and cessation of salt tectonics in the Mesozoic and Cenozoic Southern North Sea subbasins. *AAPG Bulletin*, **107**, 2169–2196, https://doi.org/10.1306/08072221105

Brennan, C., Preiss, A. and Adam, J. 2023. Three-dimensional seismic classification of salt structure morphologies across the Southern North Sea. *AAPG Bulletin*, **107**, 2141–2167, https://doi.org/10.1306/08072221136

Bulat, J. and Stoker, S.J. 1987. Uplift determination from interval velocity studies, UK southern North Sea. *In:* Brooks, J. and Glennie, K.W. (eds) *Petroleum Geology of North West Europe*. Graham and Trotman, London, 239–305.

Cameron, T.D.J., Crosby, A., Balson, P.S., Jeffery, D.H., Lott, G.K., Bulat, J. and Harrison, D.J. 1992. *United Kingdom Offshore Regional Report: The Geology of the Southern North Sea*. HMSO, London.

CCC 2020. *The Sixth Carbon Budget: The UK's Path to Net Zero*. Committee on Climate Change, London.

Cohen, K.M., Finney, S.C., Gibbard, P.L. and Fan, J.X. 2013. The ICS International Chronostratigraphic Chart. *Episodes*, **36**, 199–204, https://doi.org/10.18814/epiiugs/2013/v36i3/002

Coward, M. and Stewart, S. 1995. Salt-influenced structures in the Mesozoic-Tertiary Cover of the Southern North Sea, U.K. *AAPG Memoir*, **65**, 229–250, https://doi.org/10.1306/M65604C10

DESNZ 2023. *Carbon Capture, Usage and Storage: A Vision to Establish a Competitive Market*. Department for Energy Security and Net Zero.

Doornenbal, J.C. and Stevenson, A. (eds) 2010. *Petroleum Geological Atlas of the Southern Permian Basin Area*. EAGE, Houten, The Netherlands.

Doornenbal, J.C., Kombrink, H. *et al.* 2022. New insights on subsurface energy resources in the Southern North Sea Basin area. *Geological Society, London, Special Publications*, **494**, 233–268, https://doi.org/10.1144/SP494-2018-178

Furnival, S., Wright, S., Dingwall, S., Bailey, P., Brown, A., Morrison, D. and De Silva, R. 2014. Subsurface characterisation of a saline aquifer cited for commercial scale CO_2 disposal. *Energy Procedia*, **63**, 4926–4936, https://doi.org/10.1016/j.egypro.2014.11.523

Fyfe, L.-J. and Underhill, J.R. 2023*a*. A regional geological overview of the Upper Permian Zechstein Supergroup (Z1 to Z3) in the SW Margin of the Southern North Sea and Onshore Eastern England. *Journal of Petroleum Geology*, **46**, 223–256, https://doi.org/10.1111/jpg.12837

Fyfe, L.-J. and Underhill, J.R. 2023*b*. The Upper Permian Zechstein Supergroup of NE England and the adjacent Southern North Sea: a review of its role in the UK's Energy Transition. *Journal of Petroleum Geology*, **46**, 383–406, https://doi.org/10.1111/jpg.12843

Glennie, K.W. 1990. Outline of North Sea history and structural framework. *In:* Glennie, K.W. (ed.) *Introduction to the Petroleum Geology of the North Sea*. Blackwell Scientific Publications, Oxford, 34–77.

Glennie, K.W. and Boegner, P.L.E. 1981. Sole Pit inversion tectonics. *In:* Illing, L.V. and Hobson, G.D. (eds) *Petroleum Geology of the Continental Shelf of North-West Europe*. The Institute of Petroleum, London, 110–120.

Gluyas, J.G. and Bagudu, U. 2020. The Endurance CO_2 storage site, Blocks 42/25 and 43/21, UK North Sea. *Geological Society, London, Memoirs*, **52**, 163–171, https://doi.org/10.1144/M52-2019-47

Grant, R.J., Underhill, J.R., Hernández-Casado, J., Jamieson, R.J. and Williams, R.M. 2019*a*. The evolution of the Dowsing Graben System: implications for petroleum prospectivity in the UK Southern North Sea. *Petroleum Geoscience*, **27**, https://doi.org/10.1144/petgeo2018-064

Grant, R.J., Underhill, J.R., Hernández-Casado, J., Barker, S.M. and Jamieson, R.J. 2019*b*. Upper Permian Zechstein Supergroup carbonate-evaporite platform palaeomorphology in the UK Southern North Sea. *Marine and Petroleum Geology*, **100**, 484–518, https://doi.org/10.1016/j.marpetgeo.2017.11.029

Grant, R.J., Booth, M.G., Underhill, J.R. and Bell, A. 2020. Structural evolution of the Breagh area: implications for carboniferous prospectivity of the Mid North Sea High, Southern North Sea. *Petroleum Geoscience*, **26**, 174–203, https://doi.org/10.1144/petgeo2019-100

Griffiths, P.A., Allen, M.R., Craig, J., Fitches, W.R. and Whittington, R.J. 1995. Distinction between fault and salt control of Mesozoic sedimentation on the southern margin of the Mid-North Sea High. *Geological Society, London, Special Publications*, **91**, 145–159, https://doi.org/10.1144/GSL.SP.1995.091.01.08

Hannis, S., Bricker, S., Goater, A., Holloway, S., Rushton, J., Williams, G. and Williams, J. 2013. Cross-international boundary effects of CO_2 injection. *Energy Procedia*, **37**, 4927–4936, https://doi.org/10.1016/j.egypro.2013.06.404

Heinemann, N., Wilkinson, M., Pickup, G.E., Haszeldine, R.S. and Cutler, N.A. 2012. CO_2 storage in the offshore UK Bunter Sandstone Formation. *International Journal of Greenhouse Gas Control*, **6**, 210–219, https://doi.org/10.1016/j.ijggc.2011.11.002

Hollinsworth, A.D., de Jonge-Anderson, I., Underhill, J.R. and Jamieson, R.J. 2022. Geological evaluation of suprasalt carbon storage opportunities in the Silverpit Basin, United Kingdom Southern North Sea. *AAPG Bulletin*, **106**, https://doi.org/10.1306/03232221119

Holloway, S., Vincent, C.J., Bentham, M.S. and Kirk, K.L. 2006. Top-down and bottom-up estimates of CO_2 storage capacity in the United Kingdom sector of the southern North Sea basin. *Environmental Geosciences*, **13**, 71–84, https://doi.org/10.1306/eg.11080505015

Japsen, P. 2000. Investigation of multi-phase erosion using reconstructed shale trends based on sonic data. Sole Pit axis, North Sea. *Global and Planetary Change*, **24**, 189–210, https://doi.org/10.1016/S0921-8181(00)00008-4

Kolster, C., Agada, S., Mac Dowell, N. and Krevor, S. 2018. The impact of time-varying CO_2 injection rate on large scale storage in the UK Bunter Sandstone. *International Journal of Greenhouse Gas Control*, **68**, 77–85, https://doi.org/10.1016/j.ijggc.2017.10.011

Kyari, A. 2018. *Effects of Multiple Detachment Layers on Faulting in the UK Southern North Sea*. PhD thesis, Royal Holloway, University of London.

Lott, G.K. and Knox, R.W.O. 1994. 7. Post-Triassic of the Southern North Sea. *In:* Knox, R.W.O. and Cordey, W.G. (eds) *Lithostratigraphic Nomenclature of the UK North Sea*. British Geological Survey, Nottingham, UK.

Downloaded from https://www.lyellcollection.org by UK Research and Innovation (UKRI/BGS/BAS) on Aug 13, 2025

McKie, T. and Williams, B. 2009. Triassic palaeogeography and fluvial dispersal across the northwest European Basins. *Geological Journal*, **44**, 711–741, https://doi.org/10.1002/gj.1201

Newell, A.J. 2018. Rifts, rivers and climate recovery: a new model for the Triassic of England. *Proceedings of the Geologists' Association*, **129**, 352–371, https://doi.org/10.1016/j.pgeola.2017.04.001

Noy, D.J., Holloway, S., Chadwick, R.A., Williams, J.D.O., Hannis, S.A. and Lahann, R.W. 2012. Modelling large-scale carbon dioxide injection into the Bunter Sandstone in the UK Southern North Sea. *International Journal of Greenhouse Gas Control*, **9**, 220–233, https://doi.org/10.1016/j.ijggc.2012.03.011

Patruno, S., Kombrink, H. and Archer, S.G. 2022. Cross-border stratigraphy of the Northern, Central and Southern North Sea: a comparative tectono-stratigraphic megasequence synthesis. *Geological Society, London, Special Publications*, **494**, 13–83, https://doi.org/10.1144/SP494-2020-228

Pharoah, T.C., Dusar, M. *et al.*. 2010. Tectonic evolution. *In:* Doornenbal, J.C. and Stevenson, A. (eds) *Petroleum Geological Atlas of the Southern Permian Basin Area*. EAGE, Houten, The Netherlands, 25–57.

Pongtepupathum, W., Williams, J., Krevor, S., Agada, S. and Williams, G. 2017. Optimising brine production for pressure management during CO_2 sequestration in the Bunter Sandstone of the UK Southern North Sea. Paper SPE-185804-MS presented at the 79th EAGE Conference and Exhibition, 12–15 June, Paris, https://doi.org/10.2118/185804-MS

Shoulders, S. and Hodgkinson, J. 2024. A process-led approach to framing uncertainty and risk in CO_2 storage in the subsurface. *Geoenergy*, **2**, https://doi.org/10.1144/geoenergy2024-011

Smith, D.B. 1979. Rapid marine transgressions and regressions of the Upper Permian Zechstein Sea. *Journal of the Geological Society, London*, **136**, 155–156, https://doi.org/10.1144/gsjgs.136.2.0155

Smith, D.J., Noy, D.J., Holloway, S. and Chadwick, R.A. 2011. The impact of boundary conditions on CO_2 storage capacity estimation in aquifers. *Energy Procedia*, **4**, 4828–4834, https://doi.org/10.1016/j.egypro.2011.02.449

Stewart, S.A. and Coward, M.P. 1995. Synthesis of salt tectonics in the southern North Sea, UK. *Marine and Petroleum Geology*, **12**, 457–475, https://doi.org/10.1016/0264-8172(95)91502-G

Underhill, J.R. 2009. Role of intrusion-induced salt mobility in controlling the formation of the enigmatic 'Silverpit Crater', UK Southern North Sea. *Petroleum Geoscience*, **15**, 197–216, https://doi.org/10.1144/1354-079309-843

Underhill, J.R., Lykakis, N. and Shafique, S. 2009. Turning exploration risk into a carbon storage opportunity in the UK Southern North Sea. *Petroleum Geoscience*, **15**, 291–304, https://doi.org/10.1144/1354-079309-839

Underhill, J.R., De Jonge-Anderson, I., Hollinsworth, A.D. and Fyfe, L.C. 2023. Use of exploration methods to repurpose and extend the life of a super basin as a carbon storage hub for the energy transition. *AAPG Bulletin*, **107**, 1419–1474, https://doi.org/10.1306/04042322097

Van Hoorn, B. 1987. Structural evolution, timing and tectonic style of the Sole Pit inversion. *Tectonophysics*, **137**, 239–284, https://doi.org/10.1016/0040-1951(87)90322-2

Verdon, J.P., Kendall, J.M., Stork, A.L., Chadwick, R.A., White, D.J. and Bissell, R.C. 2013. Comparison of geomechanical deformation induced by megatonne-scale CO_2 storage at Sleipner, Weyburn, and In Salah. *Proceedings of the National Academy of Sciences of the United States of America*, **110**, E2762–E2771, https://doi.org/10.1073/pnas.1302156110

Williams, J.D.O., Jin, M., Bentham, M., Pickup, G.E., Hannis, S.D. and Mackay, E.J. 2013. Modelling carbon dioxide storage within closed structures in the UK Bunter Sandstone Formation. *International Journal of Greenhouse Gas Control*, **18**, 38–50, https://doi.org/10.1016/j.ijggc.2013.06.015

Williams, J.D.O., Holloway, S. and Williams, G.A. 2014. Pressure constraints on the CO_2 storage capacity of the saline water-bearing parts of the Bunter Sandstone Formation in the UK Southern North Sea. *Petroleum Geoscience*, **20**, 155–167, https://doi.org/10.1144/petgeo2013-019

Ziegler, P.A. 1988. *Evolution of the Arctic-North Atlantic and the Western Tethys*. AAPG, Tulsa, Oklahoma, 33–42, https://doi.org/10.1306/M43478C4